A THESIS SUBMITTED TO
THE GRADUATE SCHOOL OF NATURAL AND APPLIED SCIENCES
OF ÇANKIRI KARATEKİN UNIVERSITY

AN INVESTIGATION OF WATER-FLOW PRESSURE DISTRIBUTION ON DIFFERENT PIER SHAPES UNDER DIFFERENT FLOW CONDITIONS

IN PARTIAL FULFILLMENT OF THE REQUIREMENTS
FOR
THE DEGREE OF MASTER OF SCIENCE
IN
CIVIL ENGINEERING

BY

HAITHAM FADHIL SHIHAB SHIHAB

ÇANKIRI

2022

AN INVESTIGATION OF WATER-FLOW PRESSURE DISTRIBUTION ON DIFFERENT PIER SHAPES UNDER DIFFERENT FLOW CONDITIONS

By Haitham Fadhil Shihab SHIHAB

August 2022

We certify that we have read this thesis and that in our opinion it is fully adequate, in scope and in quality, as a thesis for the degree of Master of Science

Advisor : Prof. Dr. Ender SARIFAKIOĞLU
Co-Advisor : Asst. Prof. Dr. Salih YILMAZ

Examining Committee Members:

Chairman : Prof. Dr. Ender SARIFAKIOĞLU
Civil Engineering
Çankırı Karatekin University

Member : Prof. Dr. Zeliha SELEK
Civil Engineering
Gazi University

Member : Assoc. Prof. Dr. Cihan DOĞRUÖZ
Civil Engineering
Çankırı Karatekin University

Approved for the Graduate School of Natural and Applied Sciences

Prof. Dr. İbrahim ÇİFTÇİ
Director of Graduate School

I hereby declare that all information in this document has been obtained and presented in accordance with academic rules and ethical conduct. I also declare that, as required by these rules and conduct, I have fully cited and referenced all material and results that are not original to this work.

Haitham Fadhil Shihab SHIHAB

ABSTRACT

AN INVESTIGATION OF WATER-FLOW PRESSURE DISTRIBUTION ON DIFFERENT PIER SHAPES UNDER DIFFERENT FLOW CONDITIONS

Haitham Fadhil Shihab SHIHAB

Master of Science in Civil Engineering

Advisor: Prof. Dr. Ender SARIFAKIOĞLU

Co-Advisor: Asst. Prof. Dr. Salih YILMAZ

August 2022

The pier is considered the most important part of the bridge. The pier geometry is influencing all other bridge components. The shape of the geometry affects the forces on the pier due to waterflow characteristics. Therefore, the main goal of this research is to investigate the differences in pressure and water flow characteristics using the different types of pier shapes. This goal was achieved by using the CFD ANSYS software program. The present system compares two actual pier types subjected in Iraq and optimizes the pier shape. The investigation was done based on Al-Muadam Bridge and the Iron Bridge. The aim of choosing these two types is to understand the pressure distribution and water flow behavior relative to different water velocities which enable the researcher to optimize the pier shape design. The study observed that with the increase of pier front face shape, there is a vortex will appear and the pressure will be high. The vortex line produced a score behind the pier which represents a big problem to the pier stability. To avoid this problem, the present study optimizes the pier design by adding a curve in the front face. The pier has been reduced the pressure due to separating the pressures on both sides of the pier.

2022, 71 pages

Keywords: Pier shape, CFD, Water flow characteristics

ÖZET

FARKLI AKIŞ KOŞULLARINDA FARKLI İSKELE ŞEKİLLERİNDE SU AKIŞ BASINCI DAĞILIMININ İNCELENMESİ

Haitham Fadhil Shihab SHIHAB
İnşaat Mühendisliği, Yüksek Lisans
Danışman: Prof. Dr. Ender SARIFAKIOĞLU
Eş Danışman: Dr. Öğr. Üyesi Salih YILMAZ
Ağustos 2022

Köprü ayakları, köprünün en önemli parçası olarak kabul edilir. Bunların geometrisi, diğer tüm köprü bileşenlerini etkiler. Geometrinin şekli, hava akımı özelliklerinden dolayı ayak üzerindeki kuvvetleri etkiler. Bu nedenle, bu araştırmanın temel amacı, farklı tipteki ayak şekillerini kullanarak basınç ve su akış özelliklerindeki farklılıkları araştırmaktır. Bu amaca CFD ANSYS yazılım programı kullanılarak ulaşılmıştır. Mevcut sistem, Irak'ta uygulanan iki gerçek ayak tipini karşılaştırır ve ayak şeklini optimize eder. İncelemeler, Al-Muadam Köprüsü ve Demir Köprü'ye dayanılarak yapılmıştır. Bu iki türü seçmenin amacı, araştırmacının ayak şekli tasarımını optimize etmesini sağlayan farklı su hızlarına göre basınç dağılımını ve su akış davranışını anlamaktır. Çalışmada, ayak ön yüz şeklinin artmasıyla bir girdap oluşacağı ve basıncın yükseleceği anlaşılmıştır. Girdap çizgisi, köprü ayağının arkasında, ayak stabilitesi için büyük bir sorun teşkil eden bir skor üretecektir. Bu problemden kaçınmak için bu çalışmada, köprü ayaklarının ön yüzüne bir kavis ekleyerek ayak tasarımını optimize edilmiştir. Su akım basınçının köprü ayağının her iki tarafından ayrılması nedeniyle köprü ayağına gelen basınç düşürülmüştür.

2022, 71 sayfa

Anahtar Kelimeler: Köprü ayağı şekli, CFD, Su akış özellikleri

PREFACE AND ACKNOWLEDGEMENTS

I would like to thank my thesis advisor, Prof. Dr. Ender SARIFAKIOĞLU for her patience, guidance and understanding.

Haitham Fadhil Shihab SHIHAB
Çankırı-2022

CONTENTS

LIST OF SYMBOLS

a3	Kinetic energy correction coefficient
Ab	Net area under bridge (sq. ft. or m^2)
B	Width of top of embankment at bridge abutment (ft. or m)
C	Discharge coefficient
Db	Height of low chord from mean stream bed elevation (ft. or m)
H	Height
Lc	Length of bridge opening between abutment faces (ft. or m)
Q	Discharge
Q	Studied discharge (cfr or m^3/s)
V	Velocity
V/Vc	Relative velocity
Y	Coordinates in both sides of flow
Y3	Depth of outflow at cross department 3 (ft. or m)
Z	Depth

LIST OF ABBREVIATIONS

CF	Plus
CFD	Computational fluid dynamics
FSI	Milligram
IAC	Divide
SST	Kilogram

LIST OF FIGURES

LIST OF TABLES

1. INTRODUCTION

River flow matters and the related complications in a hydraulic engineering field of study, like the effect of impact and interaction of structurethat is fluid on piers of bridge, impact of water flow technique on the bie of the bridge, riverbed deformation, dredging and flooding are one of the main themes in the development of any country. In hydraulic engineers and designers, the flow field around bridge pier considered a key area of interest (Carnacina *et al.* 2019).

Many reasons have been reported of bridge failures such as the flood events, piles undermine and scour around bridge piers. About 5% of the failures cost of bridge damages caused by piles undermine. Furthermore, the after catastrophe repair was negatively affected due to bridge damage. An analysis of 143 bridge failures during the period from 1961 to 1975 and found that 45% related to the scour around bridge piers. Evaluating their structural response and constructional stability is very important to the safety of bridges (Shrestha 2015).

The bridge design is usually associated with the idea of an open channel flow state; in addition, the flow mode can shift to water pressure flow if the lower edge of the bridge deck is totally or partially submerged throughout a major flood. Walls and floor effects of the river can be neglected in large river cross sections and bridge deck elevation. However, a combination of such geometry with submergences of the bridge deck is of limited practical interest (Wang *et al.* 2015). For the design and evaluation of river bridges, the most consideration occurs when the free surface prevents one from applying direct models of fluid structure interactions derived for unbounded domains. The reflection of the failure and damaged reflected on the repair cost (Wang *et al.* 2015). It can be classified on direct cost related to repairing river bridges damaged by flood. Nevertheless, indirect cost considered due to business disruption and predicted to be exceeding five times the cost of direct repair. While design, planning, and building phases of the bridge are wisely calculated to achieve its application; piers repairs and protection from flow effect is given less importance than the structure will have. A maintenance strategy is required to avoid the problem of failure and the excess expenses

during the life of the bridge. Figure 1.1 explains the problem of water flow around bridge piers and its consequences such as bridge failure. In order to develop a successful bridge, the successful plan must be taking in consideration established on the design procedure, involving the design method of bridges, maintenance program and construction methods. All variables will lead to a long life of structures.

Figure 1.1 Bridge in India (Over the Gaula river) (Shrestha 2015)

1.1 Action Mechanism on the Bridge Piers

When the water flow affects the bridge pier, the pressure of the influx stream takes into account the fluid structure interaction. The dynamic interaction of structures that vibrate horizontally when in contact with one of two sides of water and the pressure effect of the hydrodynamic loads, vibration periods, and seismic reactions of structural water systems, including higher mode effects, occur. Assessing the consequences of the risk related with the possibility of water flow and the system of crossing the stream as a tool to develop site-specific design criteria. This assessment take into account capital cost, environmental hazards, and possessions influences on human life. The pier spacing and direction should be implemented by the hydraulic designer and the shape should be designed to minimize flow turbulence and possible impacts (Jalal 2019).

The foundations of the pier must be designed in such a way as to avoid damage due to wash out without preventive measures. Aghaee and Hakimzadeh (2010) made a simulation of turbulent flow around a circular pier based on the connection of velocity and pressure. Also, they investigated the nearby the pier vortexes by applying the calculation of Reynolds-averaged Navier-Stokes and by using the Navier-Stokes space-averaged calculations. There aren't many systematic studies have been performed on the pressure of the flow of water on the pier taking into account the effect of the impact. The fluid-structure interaction on piers considered a crucial issue in this studies (Aghaee and Hakimzadeh 2010).

The water flow affects the pier for a bridge and the impactig procedre around the pier resultig from the flow can be categorized into two sections: the impact moment on the bridge pier and the water flow surrouding the pier after the collision. The flow velocity quickly affected once flow impacts pier. In this case, a large amount of water moves forward besides the piers two sides walls, but some of the water flows back or halt the flow because it was blocked by the pier, as presented in Figure 1.2 (a) (Wang *et al.* 2015).

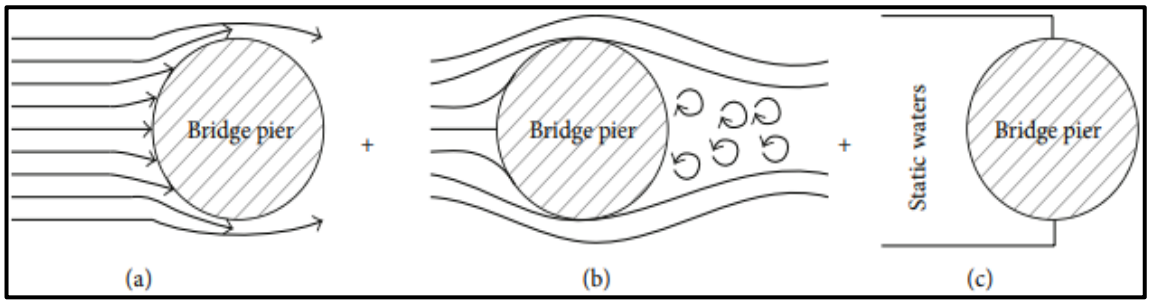

Figure 1.2 Graphic vision of flow forces on bridge pier (Wang *et al.* 2015)

Therefore, the flow influences on callad water hammer effect, pier be exposed to the momet impact effect results a fluid pressure impact with larger magnitude than the effect of static fluid pressure which produced on the pier. The water flows around the pier after the impacts area on the bridge pier, as presented above in Figure 1.2 (b). The front face of pier has greater pressure, also lower pressure happens on the back side of pier.

1.2 Problem Statement

The water flow forces on the bridge piers are very complex function of the pier shape. The amount of water flow forces generated by an object depends on the flow behavior on the shape of the object. for that, optimizing the shape represents the crucial case in pier design (Chen *et al.* 2021, Carnacina *et al.* 2019). The complex dependencies of pier shape, flow conditions and inclinations can be expressed by the water flow conditions which they considered as the hydrodynamic loads to all model related the complex dependencies (Nasim *et al.* 2019). Therefore, the standard approach for pier design optimization depends on the flow conditions of the hydrodynamic model (Jalal 2019).

These forces concern about the working parameters in the pier which represent quantities that can be considered a risk assessment on the bridge pier. The total construction get effected by the dramatic influence on the construction structure of the pier and the bridge. The reason for this phenomenon is the hydrodynamic characteristics change on the pier which is determined from the shape of the pier design. The main problem is how to decide which shape of the piers is suitable to reduce the influence of water stream and fluid-structure interaction on the bridge pier. It is a major challenge due to reflection of many flow effects and behavior round the pier correlated with the fluid-structure coupling influence.

1.3 Research Objectives

The essential purpose of this study is to examine the flow structure around the bridge piers. The effects of columns shape on flow structure round bridge pier are planned to be study in details, to accomplish this objective, the pier particular objectives are proposed:

a) Comprehensive comprehension of the flow structure idea around bridge piers such as water stream flow behavior and pressure

b) To investigate the pressure and velocity differences in different surface levels around the piers.

c) Analyzing and comparing the flow effect based on different bridge piers shape

1.4 Organization of Thesis

This Project is planned to involve five chapters. The 1st chapter is an introduction to pier effects and the failures based on previous studies, that contain a statement of the problem, overview study, objective of the study. The 2nd chapter talks about studies close or related to this study. The 3rd chapter is presenting the approaches and techniques of this study. Chapter 4 presents the collected results and the last chapter is 5th chapter that talks about what concluded from the study and recommendations.

2. LITERATURE REVIEW

Abutments and piers are considered as the essential accessories of the bridge because they hand grip the surface of the viaduct. The special geometric of the viaduct pier that influences the constancy of bridge know the sum of backing it offers, mostly throughout the overflow (Type and Elevation 2016).

The height of the upper part of the water from the pier causes a deficient In terms of the bridges impact, compressibility, as well as leads to cleaning work. Figure 2.1, plan and perspective visions of bridge down cleaning work is presented. Slacks that have no velocity occur at the top of the pier. In addition to whirlpool pointing which make scouring about pier are shown in Figure 2.1.

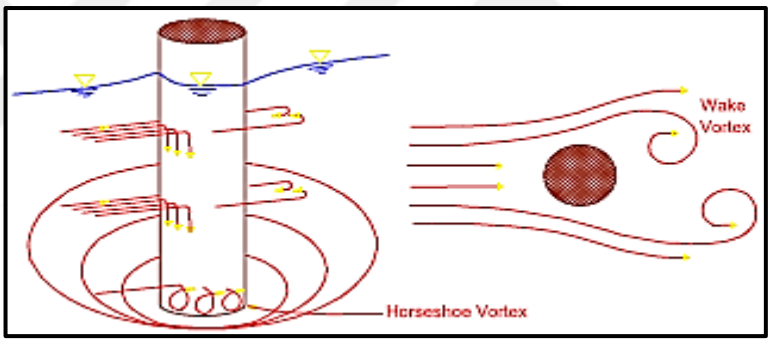

Figure 2.1 Around a cylinderical pier, there are horseshoe and wake vortices (Ipa and Di 2017)

The obstruction created by the piers and abutments of the bridge an extreme velocity in the water level at the top of the bridge. The size of the obstacle is determined by the geometric properties of the actual pier, the position within the tubes piers, and the volme of the flow, and reducing proportion, of conduit. Remission proportion, can be known as proportion among width of the pier, b, and conduit width hydraulic influences are climacteric in the resolve of the bridge framework. Numerous researches has been done with appreciation of the hydraulic effects of bridge pier to make decisions correctly (Jalal 2019). In Figure 2.2, water standard of downstream and upstream the bridges is presented. The blue bar representing the true current profile of the tumefaction is on the upper. At the junction of the bridge, the water level and the water-

raising velocity decrease due to stagnation. Y1 and Y3 designate upstream and downstream water standards, in sequence. The red color as a head bar represents undisturbed water standard (without bridge case) (Suribabu *et al.* 2011). The degree of power and head damage bar can also be seen in the Figure 2.2.

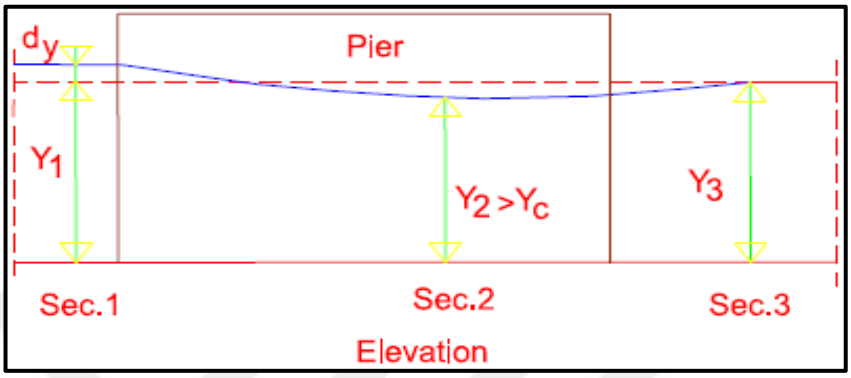

Figure 2.2 Diagram of the stream outflow congested because of the bridge (Suribabu *et al.* 2011)

On simplified piers, the effect of the horseshoe vortex is considered weak, and basically illogical hydraulic effects are expected to move the friction and sedimentation phenomena at the lowest part of the piers (Ramos *et al.* 2016). Mirali Mohammadi (2008) introduced a two-dimensional mathematical hydraulic theory to discover the dynamics properties of alluvial water flows round bridge piers. He deduced that their concept relates to the scouring mechanism of piers that refers to weak horseshoe vortex system. It is important for straight or curved prism channels, including bridge piers, to understand shear stress's lateral distribution (Mohammadi 2008).

The simulation in the study is optimized using Computational Fluid Dynamics (CFD) program. Figure 2.3 shows the width of the pier plan, the direction of flow, the geometry of the channel and the condition of the berth in the channel. In this figure, B and b/2 represent the width of the waterway and the distance between the pier and the wall, correspondingly. The pier is in situ in a symmetrically rectangular channel. In the simulation, the situation of the symmetric pier is set, and the remission ratio is defined as the ratio between the width of the pier and the width of the channel.

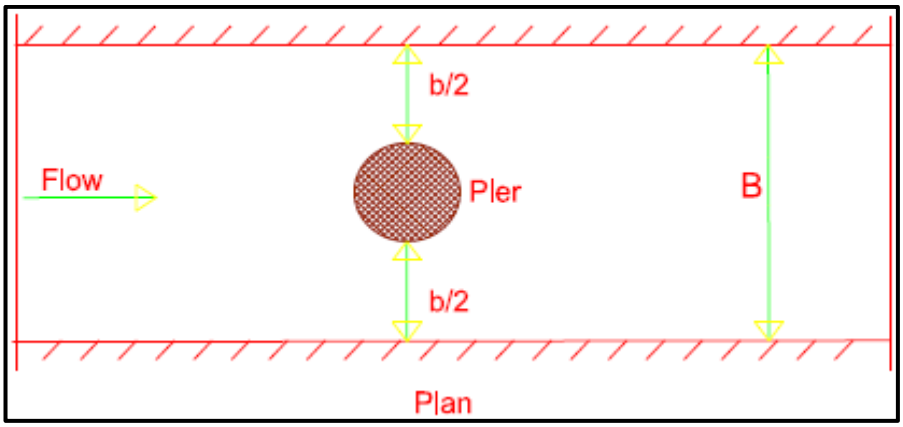

Figure 2.3 Plan view of the pier (Ipa and Di 2017)

Numerical studies are made into the traction properties of the bridge pier. Experimental studies carried out before which are the 'height of stagnant water' and traction properties of bridge piers under provisions of sub-climate outflow (Ghobadian *et al.* 2018).

Suribabu *et al.* (2011) determination of shape coefficient and traction coefficient of triangular piers under sub-climacteric outflow provisions (Suribabu *et al.* 2011). Moseley *et al.* (2016) correspondingly are made for evaluation. The study also sums up the interaction between piers of the bridge and In terms of comarisons, abtmets and piers of traction properties. Outflow 3D CFD program is used in the numerical simulation. Auto CAD solves solid work in three dimensions. In addition, the geometrical features of the piers (elliptical, rectangular, triangular, etc.) are investigated while using the model and comparig to previosresults (Moseley *et al.* 2016). Figure 2.4 shows the width of the pier profile in the pipeline. Y1 and Y3 refer to the water from upstrem and downstrem standards, in sequence. Y2 is the lowest point in the water standard. The value of Y2 is more than the depth of the peak. This condition gifts the precarious outflow provision (Tsutsui 2007).

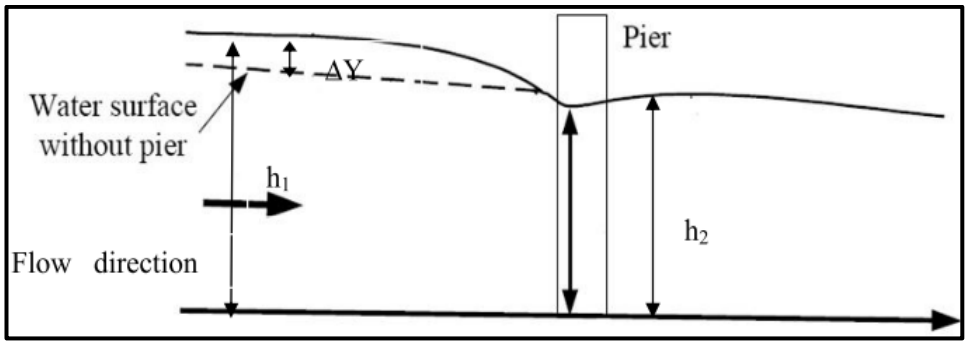

Figure 2.4 Profile view of the pier

2.1 Compression Behavior of Water-Outflow

When the overflow affects the bridge pier, another topic examined is that calculating the dynamic restriction and outgoing prevalig conditios while takig into account the fluid-structure interaction. Bouaani (2011) made the suggestion a useful formulation for research into the dynamic constraint of a frame that vibrates laterally on one or both sides in touch with water parts and improves procedures that have been simplified for the practical evaluation of vibration intervals, seismic loads, and hydrodynamic loads constraints of structural water systems including effects of the higher method (Junichi Okado *et al.* 2003). However, relatively few systematic studies have been performed on a water flow pressure pier considering the effects, especially with respect to fluid structure interactions. When the overflow affectsd the impact procedure on the bridge pier, the impactig procedure caused by the outflow on the pier can be divided into two parts: the instantaneous theresult of the flood on the pier of the bridge and the movement that the water flows around the pier after the instantaneous impact.

2.1.1 The influence of time

Moment effect of the connected system with a fluid structure the greatest possible displacement is sought at the higher end the bridge, as well as the enormous stress in the bridges lowest section (Wang *et al.* 2015). Figure 2.5 presents the change in the impact amplification factor (IAC) relative to the outflow velocity, where IAC denotes the proportion resulting from the number of constraint of a bridge pier submerged in water

outflow pressure, taking into account the movable structure relationship and the effect of flood on the bridge pillar In the transient state up to the theoretical limits of the bridge pillar under the pressure of the water flow, except for the impact effect.

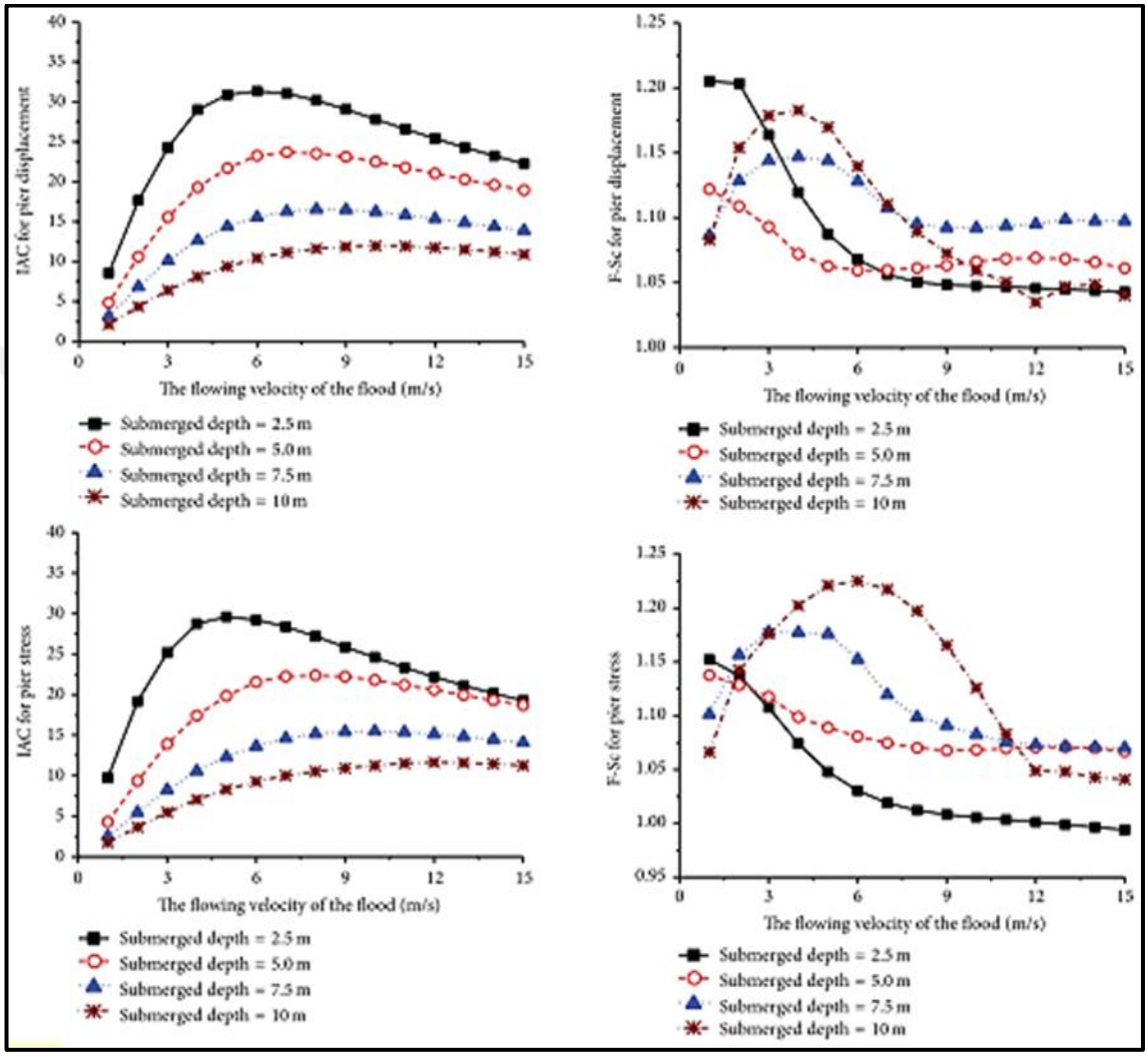

Figure 2.5 The difference of the effect amplification coefficient (Wang *et al.* 2015)

Figure 2.5 can show that, considering the displacement and pressure as the quantity of study, the IAC tends to support to some level and then decrease when the flood velocity increases slowly. Extreme IAC reduces when the ratio of the depth of the pier submerged in the flow to the total height of the pier (S-ratio) increases. When the S-ratio also rises, the outflow velocity corresponding to the extreme IAC is also greater than before. The variance IAC curves in regard to to the overflow velocity be likely to

flatten, when the S ratio goes up. is a sign that sometihing wrong. Also it shows that the IAC has a tight reationship with the flood flow the S ratio ad the velocity.

2.1.2 Effectiveness of fluid-structure

Efficiency of after a period of time, the fluid structure changes depending o the water pressure. The effect of the moment, effect on the pressure of the water flow used for the suspension bridge is coupled when the overflow affects the bridge in a steady state, the maximum displacement at the bridge piers highest point and the pressure extremes in the lower pier segment of the bridge is considered the amount studied (Alijani and Amabili 2014).

Many researchers have studied the structure of bridges under flood loading. The design of river bridges has different sides; some researchers consider the effect of structural behavior and focus on structural modelling. On the other hand some of them have focused on the dynamic aspects of water flow, containing drag forces, various parameters for fluids such as Reynolds numbers, drag coefficients, and various procedures for simulation modeling. The behavior of fluids is complex and fluid structure interaction (FSI) is a aspect that has been investigated by different scholars (Nasim *et al.* 2019, Wang *et al.* 2015). They change in the fluid structure coupling effect coefficient as a function of the current to the outflow speed, where FSI is known as a ratio of numerical values constraint of the bridge under constrction the pressure of the water flow taking in consideration the effect of the fluid structure coupling when the overflow affects the bridge pier in a steady state, to the restriction of the bridge pier under pressure water flow except for the fluid structure coupling effect.

If The F-Sc decreases when the S ratio is less than 1/2 with increasing flood rate; when the flood comes flow rate The F-Sc reaches a top speed of 6.0 m/s is directed to a have a value that is constat 1.1. If The S ratio must be at least 1/2, and the flood muust be contained flow rate does not exceed 4.0-6.0 m / s, the F-Sc will increase as theflood velocity increases, the highest value. In this case, if h / H = 0.75, the F-Sc reaches a maximum value of 1.19.

If the S ratio is h / H = 1.0, F-Sc will reach a maximum of 1.15. If the S-ratio is not less than 1/2 and the flood flow rate is greater than 4.0-6.0 cycles, the F-Sc decreases with increasing flood flow rate and eventually moves toward a static constant. In these cases, when the S-ratio is h / H = 0.75, the maximum value of F-Sc is 1.1, and when the S-ratio is h / H = 1.0, the F-Sc reaches 1.06 maximum value. Relying on this conclusion, it can be concluded that the effect of fluid structure coupling on the analytical result is small and thus can be omitted when performing a static dissection on the bridge pier.

2.1.3 Compression outflow method

By definition, compression outflow methods represent high outflow provisions. Figure 2.6 represents high flow provision where the flatness of the water upstream of the bridge collides with the low chord but the lower face is not submerged. Its provision as a slot port can be sacrificed using the first equation you need to assume successive heights in section 3 (y3) so that the discharge considered in Equation (2.1) is equal to the discharge within a suitable allowance.

$$Q = CA_b \left[2g \left(y3 - \frac{D_b}{2} + \frac{\alpha_3 v_3}{2g} \right) \right]^{0.5} \quad (2.1)$$

where:

- Q= studied discharge (cfr or m^3/s)
- C = discharge coefficient (0.5 suggested)
- Ab = net area under bridge (sq. ft. or m^2)
- y3 = depth of outflow at cross department 3 (ft. or m)
- Db = height of low chord from mean stream bed elevation (ft. or m)

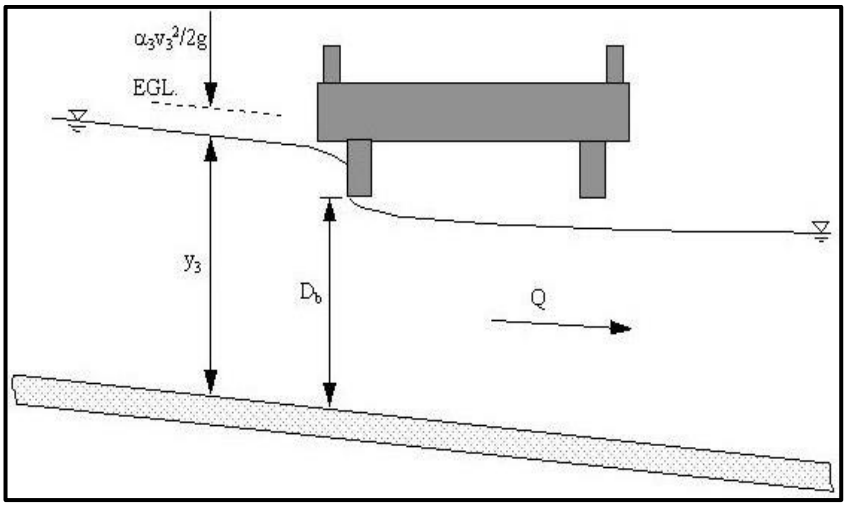

Figure 2.6 Sluice port type compression outflow

Figure 2.6 presents a bridge opening flooded with tail water less than the extra height. Equation 2.2 shows the outflow of the opening. You must assume successive inclines in section 3 (y3) so that the discharge taken into account in Equation (2.2) is equal to the torque discharge within a reasonable range.

$$Q = CA_b \sqrt{2gH} \tag{2.2}$$

where:

- C = discharge coefficient (0.8 typical)
- H = difference between energy grade at cross department 3 and water flatness at cross department 2 (ft. or m), Equation (2.3).

$$H = y3 + \alpha_3 \frac{V_3^2}{2g} - y2 \tag{2.3}$$

where:

- a3 = kinetic energy correction coefficient
- Cd=coefficient of discharge, Equation (2.4).

$$C_d = 0.104 + \frac{L_c}{b} + 0.7145 \tag{2.4}$$

where:

- b = width of top of embankment at bridge abutment (ft. or m) (see Figure 2.7).
- Lc= length of bridge opening between abutment f (ft. or m) (see Figure 2.8).

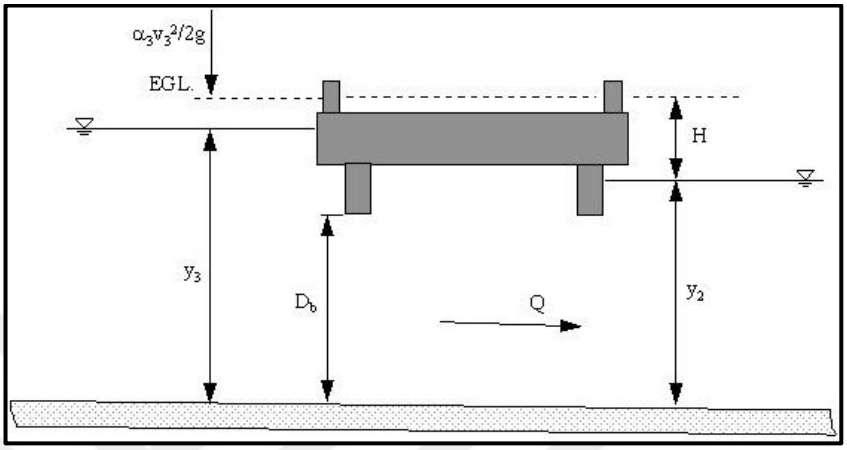

Figure 2.7 Opening kind compression outflow

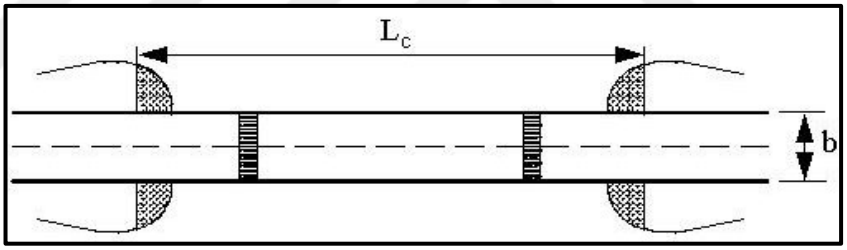

Figure 2.8 Bridge geometry for compression outflow analysis

2.2 Swirl Arround Piers

The main mechanical instruction for local scour at piers or abutments is to point the swirl. The vortex is directed around the front of the pier or pillar by the water's concentration on the up-stream face and later flow velocity. When the average movement of sediment away from the local region exceeds the mean transport of sediment away from the area, the score hole improves. The force of the swirl decreases as the scouring depth increases, lowering the transport average. Garbage will stop and the scour hole will not get any larger once balance is restored. The following is an example of a standard pier swirl:

1. Horseshoe swirl
2. Swirl your wake,
3. A bow wave,
4. Trailing Swirl.

These vortices are responsible for the holes formulation around piers. Many bridges are being harmed by this type of corrosion (Hamidi and Siadatmousavi 2018). Figure 2.9 depicts the many forms of swirl that occur around piers.

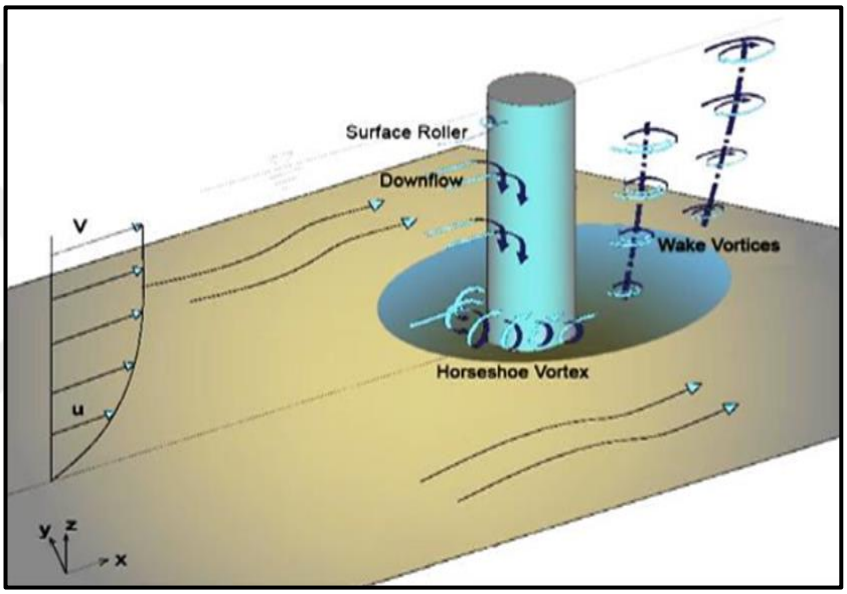

Figure 2.9 Types of swirl around piers

2.2.1 Horseshoe swirl

The horseshoe swirl is the outcome of 3D separation of the boundary layer that coils upward in a vortex forward and alongside parts of the cylinderical pier (Melville 1975). A part of the outflow in which approaches the piers is redirected to bed and twists up for producing what is commonly represented as the "horseshoe swirl" around the front face of the structure. Because of its resemblance to a horseshoe, this swirl is commonly referred to as a horseshoe swirl. The horseshoe swirls system is shown in detail by Shen *et al.* (1969). The recession compression gradient on the structure's command edge caused by the bottom boundary layer of the oncoming outflow starts the horseshoe

swirl. That is, a change in outflow speed from zero at the bed to a specific value at the flatness results a stagnation's change compression at the structure's command edge. At the elevation of the highest velocity, the most stagnation compression occurs. The scour mechanism is controlled by a combination of the horseshoe swirl and down-outflow.

2.2.2 Wake swirl

The so-called wake-vortices are formed by the separation of the outflow at the piers' portions (Zhai 2010). The approach outflow transfers wake vortices downstream and functions like a vacuum cleaner when it removes downward material, which is subsequently carried through the downhill and horseshoe vortices (Melville 1977). A separation strip separates the wake-swirl system from any area of the pier, which is made up of unstable shear layers created during pier smoothing (Tsutsui 2007). The horseshoe and the wake wear away at the pier's remnant. The materials that are removed by these swirls are frequently redeposited downstream. With increasing distance downstream, the vortices' force decreases, resulting in a common sediment deposition downstream of piers (Aghaee and Hakimzadeh 2010, Tsutsui 2007).

2.2.3 Bow wave

When the upward outflow creates a circulation around the free flatness, bow waves are created (Melville 1977). The outflow profundity, which is the diameters of a horseshoe swirl plus the bow wave, does not dominate the scour mechanism of piers unless the outflow profundity is very small.

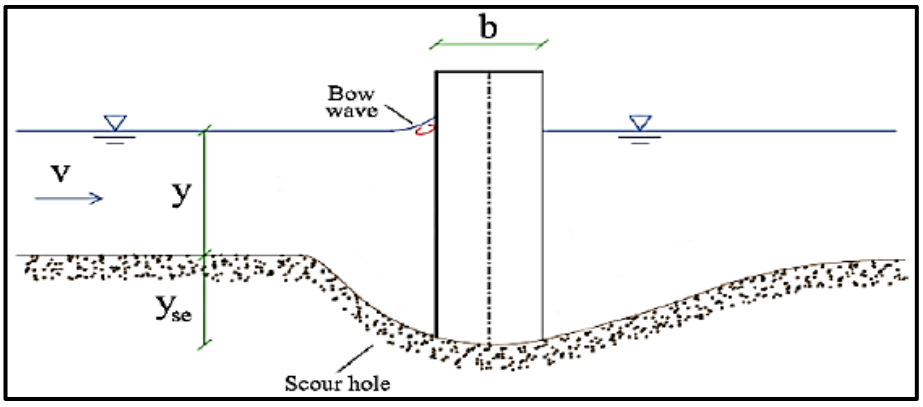

Figure 2.10 Bow wave schimatic diagram

The horseshoe swirl and the bow wave interact with each other when the outflow depth falls (Lee 2018). The bow wave causes the horseshow swirl to weaken, resulting in a reduction in scour profundity. In Figure 2.10, the bow wave at piers is seen. Where y is the average outflow depth and y is the extreme equilibrium scour profundity.

2.2.4 Trailing swirl

Normally, the vortex appendage system only appears on totally submerged piers. It is made up of several independent vortices that are attached to the quay's top and spread downstream. When a finite pressure differential exists between two flat surfaces meeting at an angle, generally at the pier's upper end, vortices occur (Mohammadi 2008).

2.3 Scour Affacting Factors

The five parameters following have been known as factors inwhich effecting the profundity of scour thereabout a pier.

2.3.1 Pier width

The depth of the scour is directly proportional to the width of the piers. The pace of outflow through the bridge opening increases as the piers widen, ensuring continuity

and leading to scour depth safety (Richardson and Davis 2001). Shen *et al.* (1969) and Breusers (1970, 1977) investigated the efficiency of pier dimension (1977). Those who discovered shape and power of the horseshoe swirl, which are factors of pier size, are the major causes of debris. The depth of the clear pit and the length of season it takes to produce a given shear pressure ratio are proportional to the size of the pier.

2.3.2 Effect of outlow intensity

The ratio of the shear speed to the climacteric shear speed (the percentage of the mean speed of the approaching outflow (V) to the climacteric mean speed) is the measure of outflow intensity (Yang *et al.* 2018). The depth of local cleaning in uniform sediments grows almost linearly with outflow strength under clear water supply, reaching maximum velocity at lowest velocity (Yang *et al.* 2019). When the proportion Vs/V*c = 1 or V/Vc equals 1, the severe scour profundity is obtained. The initial peak is the severe scour profundity that corresponds to it. When the outflow strength V/Vc is less than 0.5, no clear occurs, however when the flow intensity is between 0.5 and 1.0, clear water scour provisions occur for both ordered and non-uniform sediments. If VNc > 1.0 (live-bed clear) or clear with the movement of the sediment, the scour depth grows practically linearly with V. When the velocity exceeds the initial speed, the organized sediment's local scour depth declines at first, then climbs to a second peak level. Because the high threshold is not tired and the sediments are organized, these changes are minor. The second increase, known as the live-bed high, occurs in the flat transitional phase of the sediment moved on the channel layer. The balance between sediment intake and output from the clear pit explains the varying scour depth with outflow density. The general conclusion was that the extreme local scour profundity in orderly sediments happins at the threshold provision for clear-water scour provisions (Topczewski *et al.* 2016, Melville 2008).

2.3.3 Effect of outflow depth

The shallowness of the outflow is measured by dividing the flow profundity (y) by the width of the pier (b). The impact of depth of the water on clarity is a contentious topic.

Ettema *et al.* (2011) demonstrated that for shallow flows, a flattening cylinder (or arc wave) emerges in front of the bridge pier, interfering with the horseshoe vortex's apparent activity owing to the reversal feeling of revolution. As the flow depth increases, the flatness roller's interference with going down the outside and lowering the horseshoe in a spiral, and the influence of flow profundity become a minor. According to Richardson and Davis (2001), outflow depth has a direct impact on clear depth. A wag, the depth of the flow, can increase the scour profundity by a factor of two or more for pier scour. Melville (2008) is a fictional character the influence of the depth of the flow with regard to the breadth of the pier is represented by the shallowness of the flow y/b. In the case of deep outflows relative to pier width, the clear depth is proportional to the pier width and separated from y in the case of narrow piers. In contrast, the free depth Q is proportionately separated from y and b for shallow outcrops compared to the pier width, whereas ds is similarly dependent on y and b for medium-depth outflows. Figure 2.11 and Table 2.1 show these directions, and scour profundity becomes distinct from the depth of the outflow whenever the proportion of outflow depth to the width of the pier exceeds 1.4 (Ghobadian *et al.* 2018).

Table 2.1 The obvious local operations on piers of bridge (Melville 2008)

No.	Pier Class	y/b	Pier Scour Dependence
1	Narrow	y/b>1.4	Ds α b
2	Intermediate with pier	0.2 ≤ y/b ≤1.4	Ds α √yb
3	Wide pier	y/b <0.2	Ds α y

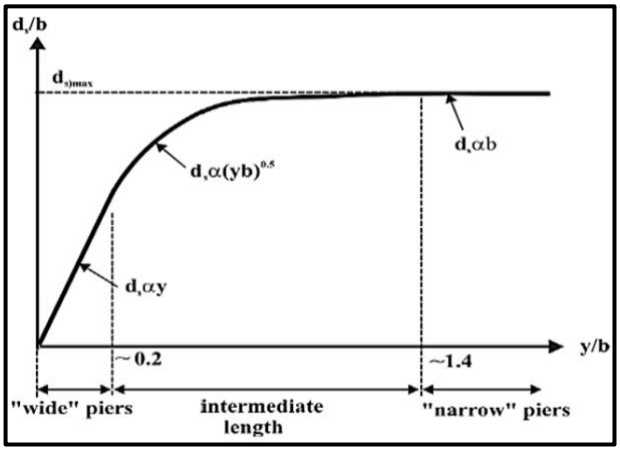

Figure 2.11 The contrast of the depth of the local scour with the shallowness of the outflow (Melville 2008)

2.3.4 The sediment size effect

The efficiency of the sizes of particle and sediment component intensity in initiating sediment movement is frequently stated as a function of outflow velocity. The influence of sediment volume on the local depth of the mesh at the bridge pier was explored by Malik *et al.* (2014). Under the clean water supply, the researchers used a pier with a diameter of 102 mm and a stream that was 1.5 meters wide. The d50 S 0.7 mm sediment causes direction ripples, and the tests may be carried out with the outflow of V without causing irritation to the upstream layer due to the approach flux. The flatbed cannot be retained for the same outflow savings with fine sand (d50 C mm). Nasim (2019) discovered that for sediment by volume, ripples often improve at shear velocities V(above 0.6V). As a result, the clean water supply was not maintained at a sufficient level to allow the silk sand to reach the same depth as the high scour. If the gg CLI is in the range of the geometric standard deviation, the sediments weren't ordered and the coarse grains preserve channel flattening but they weren't large enough to be saved from the transparent aperture where the agitation was strongest. The same examination as with non-ripple-forming sediments can therefore be carried out at clear water depths. The relative sediment roughness (b/d50) is defined as the ratio of the width of the pier (b) to the average grain size of an element of a sediment (d 50) (Melville and Coleman 2000). Local scour depth vs. sediment coarseness is depicted in Figure 2.6. The pier diameter is D, the scour profundity is Z, and the severe scour depth is measured in mm (Melville 2008, Vijayasree *et al.* 2019).

2.3.5 Effect of pier shape

One of the basic factors that acting as an important role in creation & strength of the circulation system is the pier geometry. The bridge piers are constructed in various sizes and shapes. The most known shapes used are rectangular, square, round, oblong with

beveled ends, oval, rectangular. Figure 2.12 shows a diagram vision of some forms of pier.

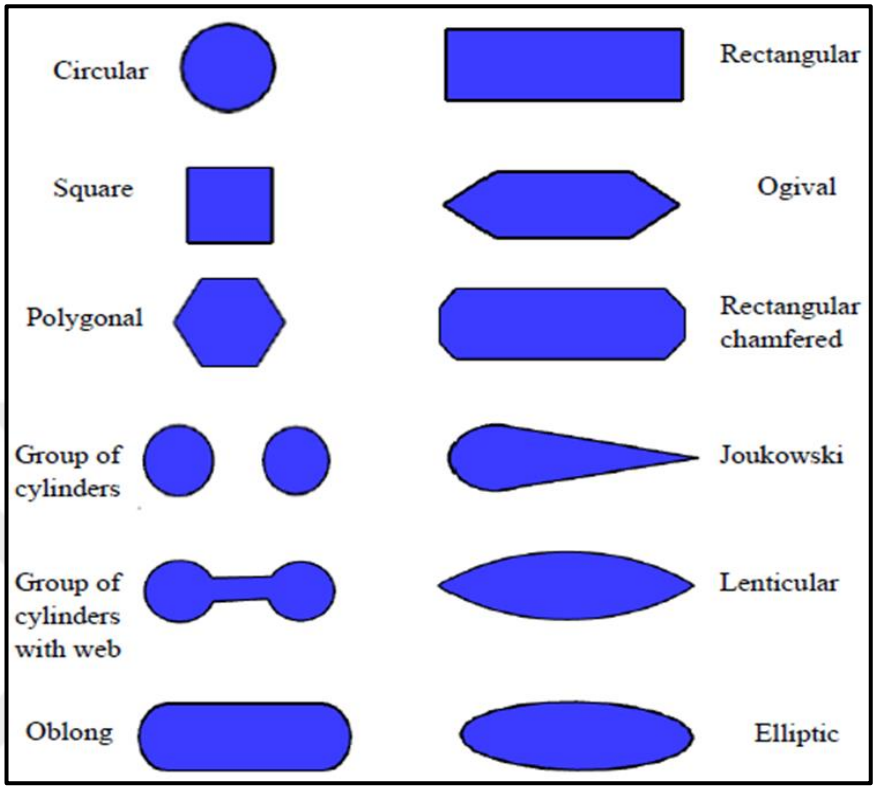

Figure 2.12 Diagram description of known pier shapes (Jalal 2019)

Several academics computed the form impact by dividing shapes of the pier into: sharp-nosed piers & blunt-nosed piers. Because the second category piers (the blunt-nosed) generate a powerful horseshoe-shaped vortex system, the scour occurs at a deep depth in the pier's nose. If this pier (the blunt-nosed) is in line with the outflow, at the weakness of the horseshoe vortex system and very deep scour occurs near the end of the estuary, then the upper pier's shape will have a strong effect on the scour's depth and the pier's length, while the shape of the lower pier will have an effect on the floor. The breadth, length, form, and alignment with outflow are all factors in pier geometry (Melville 2008).

Piers types can be divided to two kinds simple piers and complicated piers. The first type is simple piers which are the piers a containing (throughout the depth) a fixed

section. The piers with caissons, pile or slab foundations, and tapering piers are classified as complex piers. The quantity of clear was strongly influenced by the design of the piers. Streamlining the front end of a pier lessens the intensity of the horseshoe spin while also reducing clear depth. The force of the wake vortices is reduced by streamlining the downstream piers end. The multiplying correction factors express the impacts of shape & alignment on local clarity. Form variables are only essential if axial airflow can be ensured, according to the research. The advantages of the pier shape are negated by even a minor impact angle. Table 2.2 and Table 2.3 shows some possible values for the form effect in respect to the circular pier's shape. Few academics have looked at the impact of pier alignment. The outflow impact is well demonstrated to be one of the most important variables altering local clarity near bridge piers.

Table 2.2 Suggested values for the pier shapes

Shape	**Pier shape factor**								
	1/b	**Tison 1940**	**Laursen *et al.* 1956**	**Chabert *et al.* 1956**	**Garde 1961**	**Laursen 1963**	**Dietz 1973**	**Neil 1973**	**Maatooq 1999**
Circular	1	1.0	1.0	1.0	1.0	1.0	1.0	1.0	
Round nose	4		1.0		1.0	1.0	0.85	1.0	0.87
Rectangular	4		1.11		1.11	1.11	-	1.33	
Sharp nose	4	-	-	-	-	-	0.76	0.8	
Lenticular Nose	4	0.59		0.73		0.76			
Elliptical	4		0.83			0.83	0.8		
Joukowski	4			0.86		0.86			
Rectangular chamfered	4						1.01		

Table 2.3 Correlation factor for outflow alignment

0 / **1/b**	**Flow alignment (K0)**				
	0	15	30	45	90
4	1	1.5	2	2.3	2.5
8	1	2	2.75	3.3	3.9

12	1	2.5	3.5	4.3	5

2.4 Fluent Models

Optimization of the CID perturbation pattern is required to select the appropriate undoing method. Advances are urgently needed in the prediction of turbulent outflow flux with strong reversible pressure gradients and the interaction of separation with boundary layer outflow. In computational methods, the Reynolds average (RANS) methodology is the most widely employed practical method due to its reliability and height accuracy, and the low computational fluid dynamics (CFD) method (Atkins 2015).

As mentioned earlier, it is assumed that piers and abutmets produce a rise in water level occurs when outflow remission begins at the upstream of the piers. Traction forces on the piers dissipate energy in the outflow, and the replenishment of the outflow causes the water level in front of the piers to rise. The degree of the tensile force on the outflow is the same to the piers force, but in the opposite direction path. In addition, traction contains frictional traction and compressive traction. By making use of the momentum equation, the total traction force can be found. A plentiful alarge number of studies have been made in relation to properties of traction and the piers of bridge. Charbeneau and Holley (2001) conducted a lag study on bridge piers and traction properties. Traction properties of different cladding frame geometries with remission rates of 0.33 and 0.4 for critical outflow provisions were studied (Suribabu *et al.* 2011).

Chang and Constantinescu (2015) carried out an an investigation into the traction properties cylindrical in shape pillars with various gap collar derivatives. Several studies that are directly connected to the topic of our research and are outlined briefly below. Charbeneau and Holley (2001) carried out an experiment the effects of standing water, traction forces, and changes in water parameters on both the top and course of piers for bridges. In this work in progress, various the dimensions of artificial under the bridge piers in the laboratory effect of the critical outflow. Changes can be noticed in

the water parameters and thus in the traction properties of the piers. The study includes the examining the influence of the drag coefficient of piers of measurement by contrasting the results of the laboratory and the prototype. Also, the study compared thier test results with prior research, and then improving the according to the proposed formula change of water standard and the number of Frode. The research cleared that the stagnant water equation can be used to calculate the water standard. Ettema *et al.* (2011) conducted a study by evaluating the traction properties of piers of various forms that has the same expected area. They inspected the piers (there are two of them) different remission rates under the provisions of subcritical outflows. Discharges are measured and traction forces, traction coefficients and changes related to the Froude number was studied. Round, rectangle with curved ends, elliptical, rectangle with curved ends, treble nose and tail (2.5 cm and 3.5 cm), oblong, rhombus and rectangular and their hydraulic data were examined. Also they used stated forms for calculating the influence of remission quantities of 0.33 and 0.40.

The effects of stagnant water Aura have been transmitted and then compared to the stagnant water equation with the attempt to improve the equation. Chang and Constantinescu (2015) similarly, experiments were performed on under subcritical flow, trianglar piers provisions to obtain the drag from ad coefficient modulus. The rectangular specimen with a piers with a triangular nose and tail was divers points of view part as the channel in wich the experimental inestigation was conducted carried out, had a steady remission ratio of 0.4. They used four different percentages of piers with a rectanguiar shape a nose with a triaglar shape and a tail. The piers have the a ssimilar thickess (6 cm); they have different lengths of rectangle shape part (4, 6, 12, 16 cm). The results showed that the coefficient of traction depending on the sitation percentage of a part of the piers. The alterations in discharge the standard of standing water in the upper part. Also, the experimental results with the y formula was compared (Ipa and Di 2017). The scholars investigated the turbulent flow of the open channel to reveal the final features of clear pit. Extending the range of previous 2D simulations, the Reynolds-Avenide-Stokes (RANS) equations and the k-perturbation closure pattern were set in the 3D sample. Several scholars intended to enhance and to use a 3-D sample to inspect clear—hole pointing about a cylindrical bridge pier. Software was

applied; Python and Java Macros software in the project was contracted to create the technigue of computation. The specimen used RANS eguations annd their application K-"perturbation sample. The numerical the research is based o an experimet laboratory tests, the study also attempts to apply the transient testing phase of all outflow fields around the pier pressure and bed shear (Jalal 2019, Saraf *et al.*, 2016).

In the research into Raisee *et al.* (2010), the purpose the goal of the research was to take a sample from the scour hole of the turbulent outflows of the open channel through the overflow. Also they used RANS formulas, using a procedure named slip-flat-top flatness. They were comparig notes obtained results of simulation with correlations of other experimental climate shear pressure and bed roughness values properties by sediment removal. Yuce *et al.* (2016) check the outflow around a submerged cylinder interested in both experimental and numerical studies. The objective of the research to calculate the free flatness geometry as well as outflow the cyllindwr pattern. The two-dimensional channel is artificially induced under sub-climate outflow circumstances with Reynolds and Freud numbers in the raging from to 5,000 and 10,000, correspondingly (Suribabu *et al.* 2011, Malavasi and Guadagnini 2003).

Numerical results of the outflow are calculated using standard turbulent samples k- “and RNG k-” and the dimensions of the free surface is studied with the VOF sample given in the Fluent code (Ipa and Di 2017, Stanford University 2004). The objective was to study relationship between the free and the plain and the wave to improve the points of division. Both the conventional k-co specimen and the transformed k-specimen are multiplied by the blending function and both specimens are added together. The blending function is defined as one in the wall range that activates the standard k-co pattern and zero away from the plain that activates the transformed k-pattern. In addition, the SST specimen contains the expression derivative attenuated by diffusion in the joint equation (Soğukpınar 2017). Scholars are trying to improve these methods by modifying the turbulent speed to calculate the turbulent shear stress transfer. In 1994, Meat enhanced the SST (Shear Stress Transfer) sample based on k-co. Uses the k-co specimen around flatness and the k-e specimen in the free shear layers. The advances mentioned make the SST k-co specimen further accurate and dependable for a larger

class of outflows than the standard k-co specimen. For these causes and the moderately high efficiency of the numerical solution, the two-equation SST k-co specimen is set asa separate technique for the body-flow numerical simulation (Saraf *et al.* 2016). Therefore, this technique was employed in this study because the properties of combining both the standard k-co specimen and the features of the standard k-a model. In addition to that, the specimen equations act appropriately in both the wall and far regions.

3. MATERIALS AND METHODS

3.1 Design of Study

The design of study are shown in Figure 3.1.

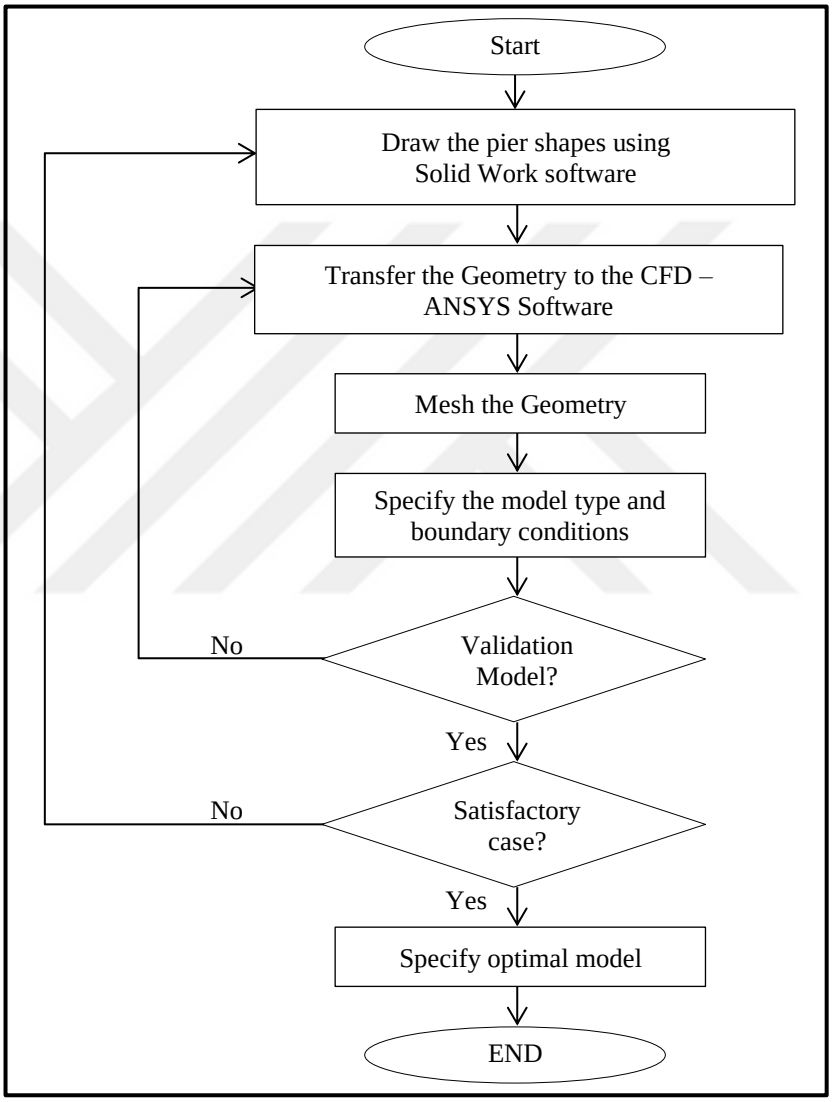

Figure 3.1 Research flowchart

3.2 Create the Geometry

In order to create the bridge pier shapes geometry, there are steps to do that as in below:

Step 1: Specify the bridge pier shapes. In this section there are two types of piers have been specified from Iraq as a case study (Figure 3.2, Figure 3.3).

Figure 3.2 The first case study (Bab Al-Muadam bridge)

Figure 3.3 The second case study (The iron metal bridge)

Step 2: Compare the bridge pier shapes response.

This result will be copied and sent to SolidWork software to draw the water shape geometry.

3.3 Plot the Geometry

Model building in SolidWorks usually begins with a 2D sketch and is then the model will be developed to different geometry. The drawing consists of geometric shapes such as points, lines, arcs, and cones. The SolidWorks steps to create the geometry are as in below:

Step 1: Start the solid works software program and choose a (Part File) for each part of the bridge pier shapes of formula one car race.

Step 2: Input (*x, y,* z) design data points created by water tool software. By using the curve from the insert of menu bar, the interface of (x, y, z) data dialog box will appear. All the gained data collected from the previous steps will be inserted in this box. This step will provide the SolidWork software the dimension of bridge pier shapes section. The connection between points of the section will give the surface curve. Figure 3.4 show the results of water design.

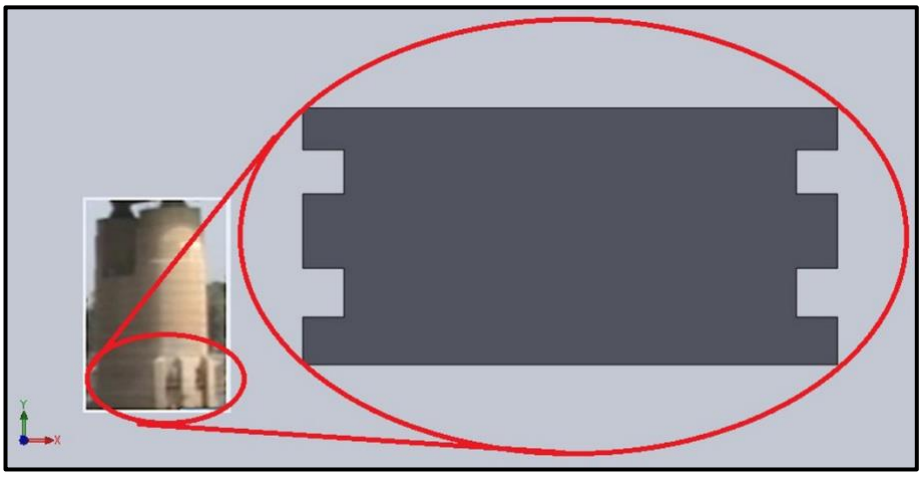

Figure 3.4 Plot of the iron metal bridge section

The bridge pier shapes section will extend by using the extruded in features bar. This feature will give the length of the bridge pier shapes as shown in Figure 3.5.

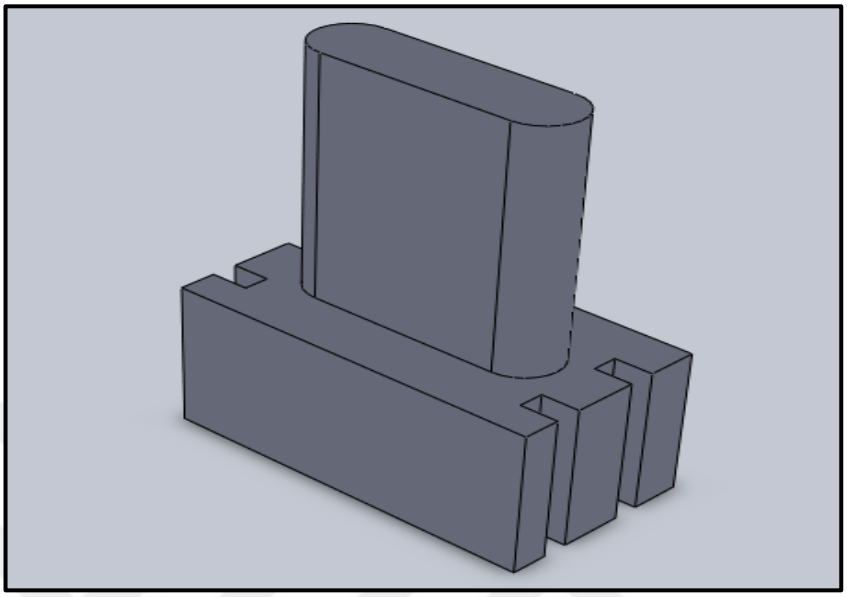

Figure 3.5 3D plot of the iron metal bridge pier shapes

Using the same standard simple shape geometry of the bridge pier the second case study will be drawn as shown in Figure 3.6 and Figure 3.7.

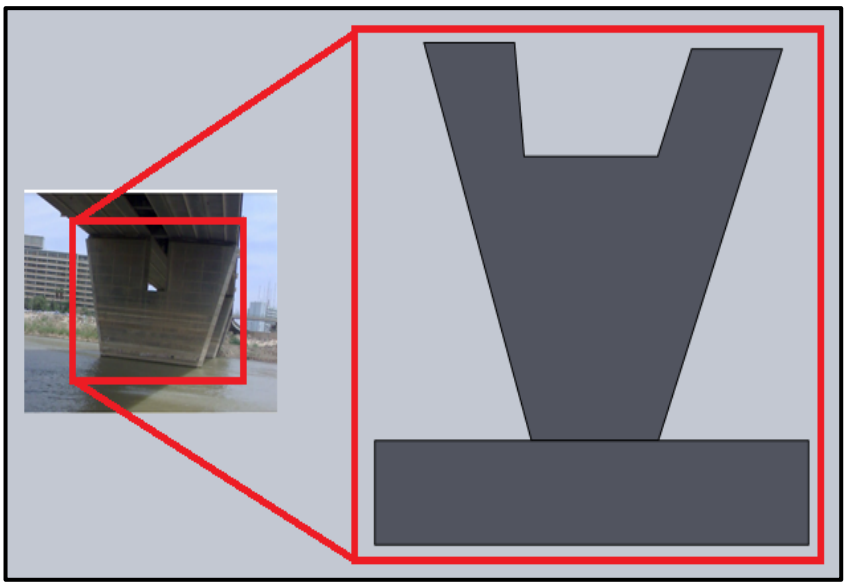

Figure 3.6 Plot of Bab Al-muadam bridge section

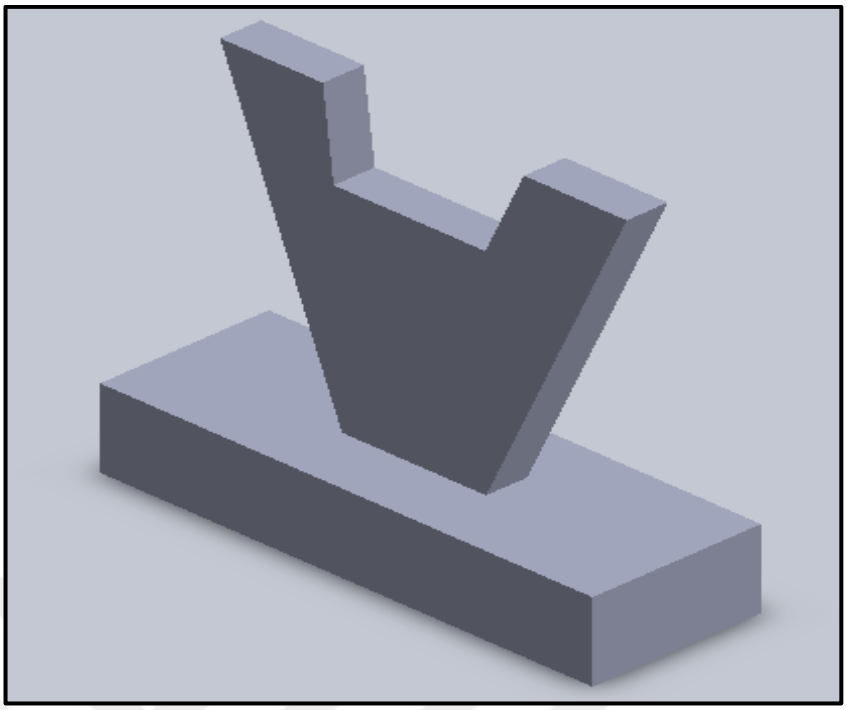

Figure 3.7 3D Plot of bab al-muadam bridge pier shapes

The presented pier shapes will the base of the bridge pier which will be used in the first step of simulation process to investigate the part features of flow around them and investigate the differences.

Step 3: Convert the geometrical draw bridge pier shapes to IGS extension file.

3.4 ANSYS Program Simulation

For studying the behavior of water flow, computational fluid dynamics is capable to analyze problems related to fluid flow. ANSYS simulates the chosen states with surfaces defined by the boundary conditions. The Fluid Flow (Fluent) option will be the specific part of ANSYS (Cakir 2012).

The steps below will provide the sequence of simulation:

Step 1: Transfer the Geometry

This step will provide the ANSYS – FLUNT software by the shape geometry from SolidWork step. The IGES file will be able to deal with the ANSYS tools. The drawn shape geometry in Design Modeler of ANSYS Workbench shown in Figure 3.8 below:

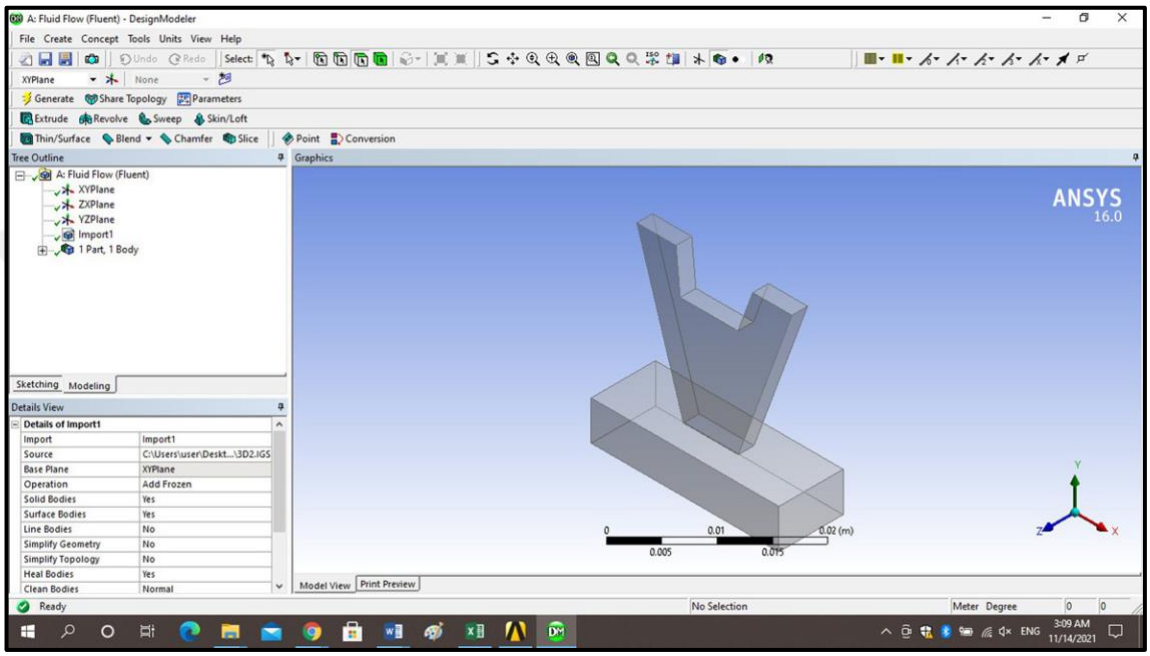

Figure 3.8 Shape geometry in design modeler of ANSYS workbench

Step 2: Meshing the Geometry

Meshing the geometry is divided the entire face into innumerable small finite number of elements. Meshing produce to us a scope to investigate the behavior of different parameters (for example pressure, velocity etc.) at each of these elements. The steps for creating the mesh are shown in Figure 3.9 and Figure 3.10.

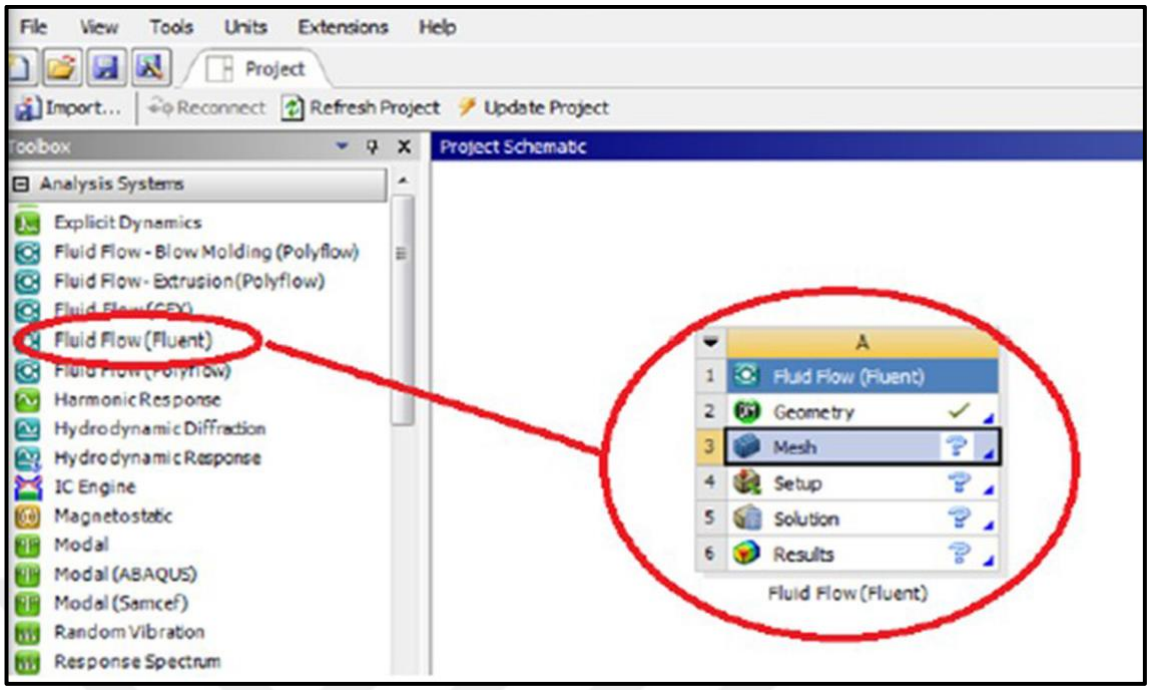

Figure 3.9 Specify mesh process

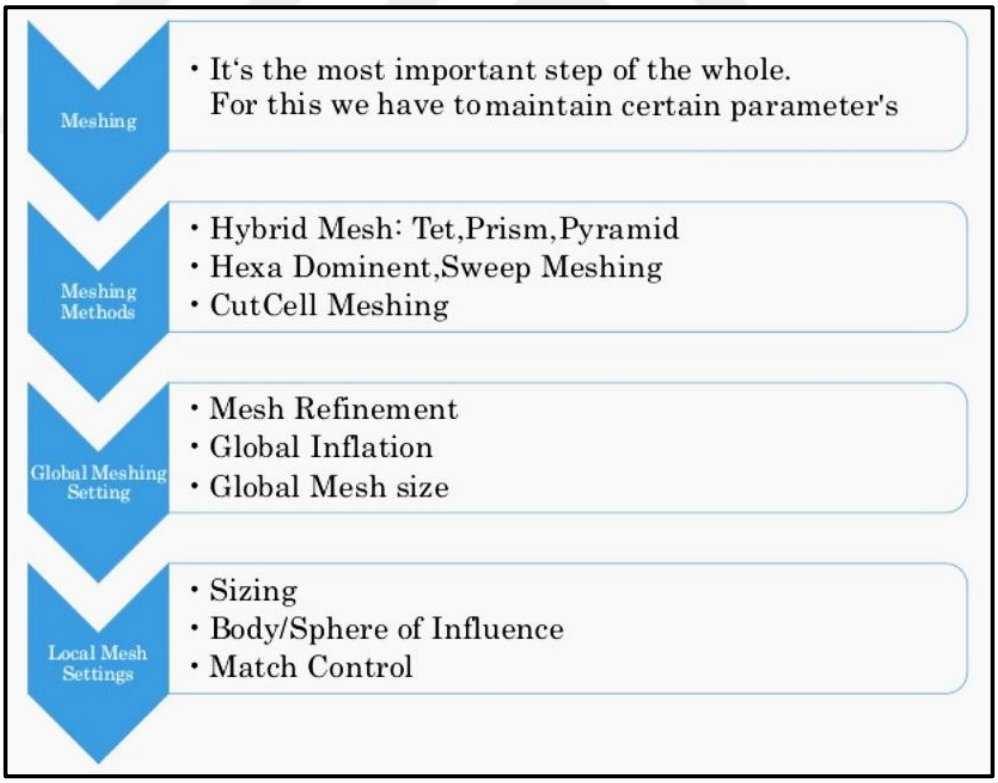

Figure 3.10 Mesh steps

The mesh process of the water applied on the flow domain based on 3-D mesh elements shape. The triangular choice observed in Figure 3.11.

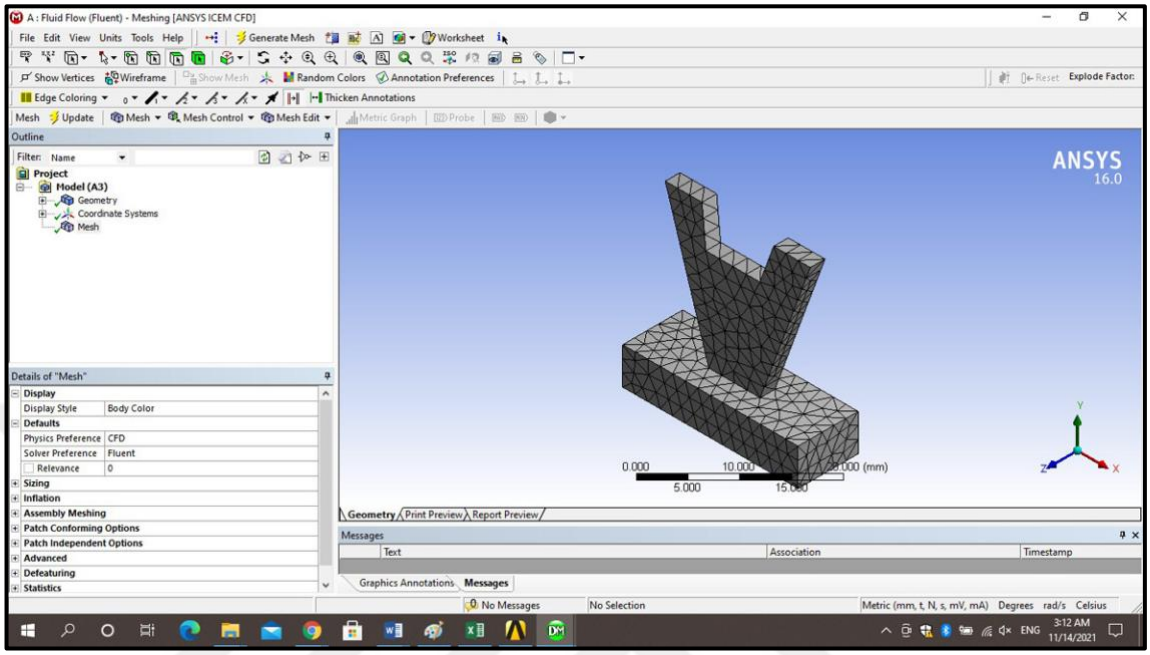

Figure 3.11 Mesh results

Size functions allow us to control the size of grid element edges for geometric edges and for interlaced faces or volumes. To determine the degree of mesh associated with higher quality, the control graph notes the item metrics related to the item number. Mesh quality statistics represents a good way to measure mesh health (Ramos *et al.* 2016, Tun and Onn 2018). In the ANSYS mesh, there are a number of mesh quality statistics at the press of fingertips. A fast and easy way to check the mesh is the minimum orthogonal quality stats which should be more than 0.1 and maximum deviation which should be less than 0.95 as presented in Figure 3.12 (Honarmand *et al.* 2019).

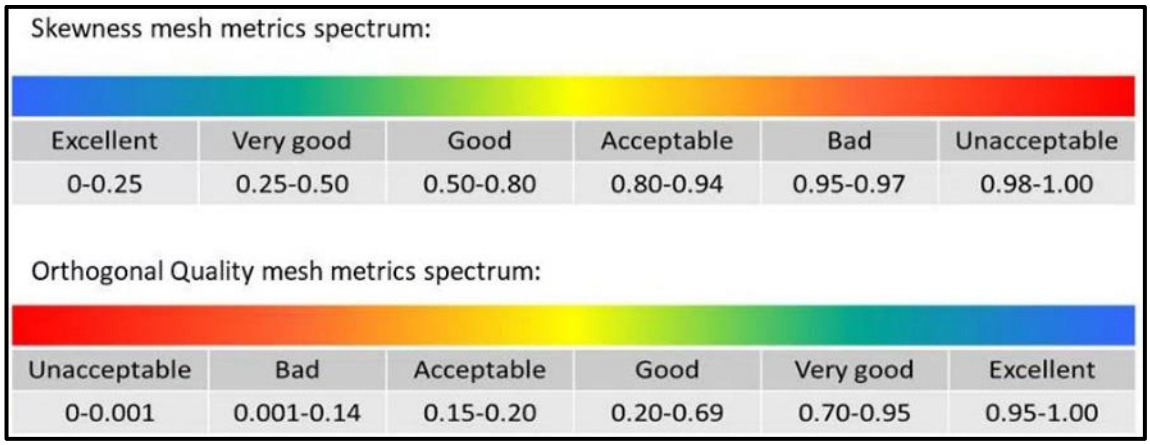

Figure 3.12 Mesh quality

In order to control the mesh quality, the use of control table specify the size and type of mesh as shown in Figure 3.13.

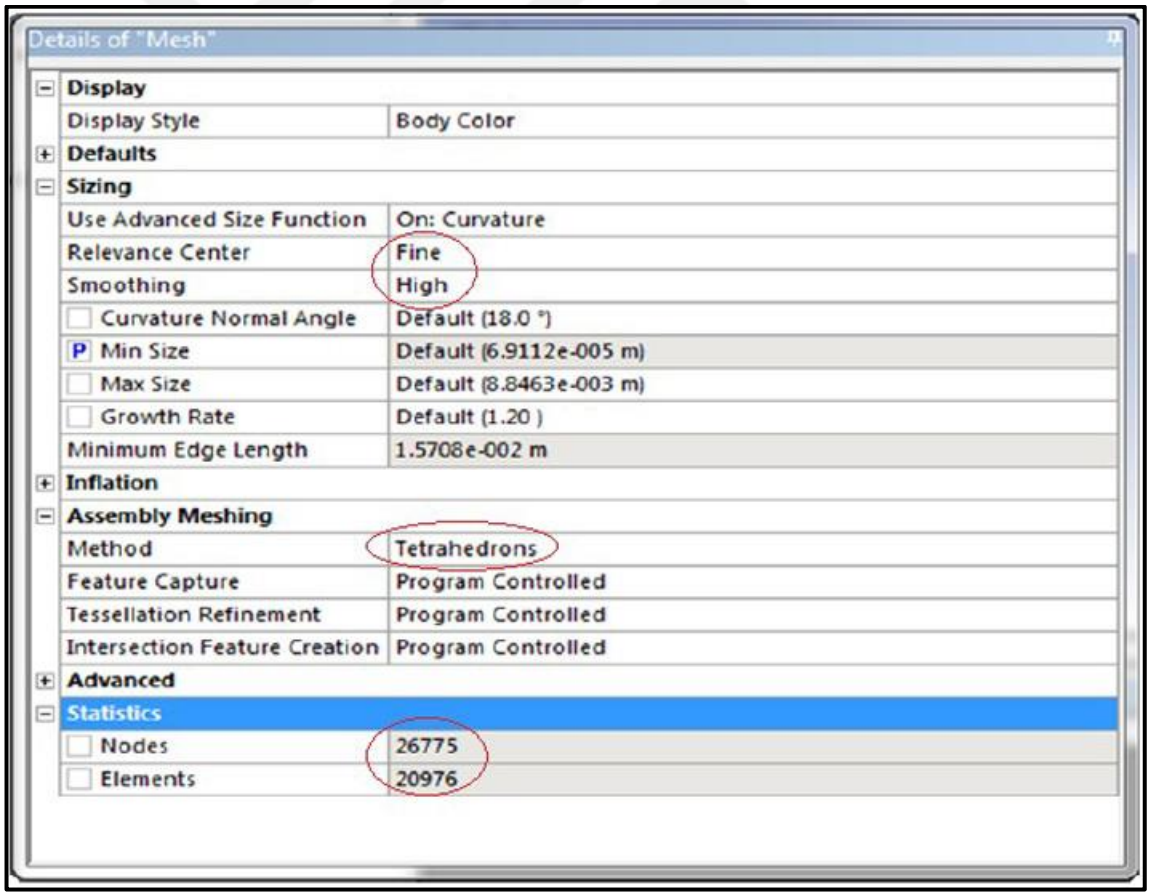

Figure 3.13 Control parameters in meshing the geometry

Step 3: Setting Up the CFD Simulation

The computational mesh geometry of the bridge pier shapes Formula One race car will convert to set up step of CFD analysis in ANSYS Fluent. The procedure of this step describes in the follow of water in bridge pier shapes tasks:

1. Start ANSYS fluent

In the ANSYS Workbench Program Diagram, when interring the Setup cell to show the context menu, the ANSYS Fluent is first started, the Fluent Launcher is showed, the ANSYS Fluent start-up options will appear as in Figure 3.14 (Sunny *et al.* 2017).

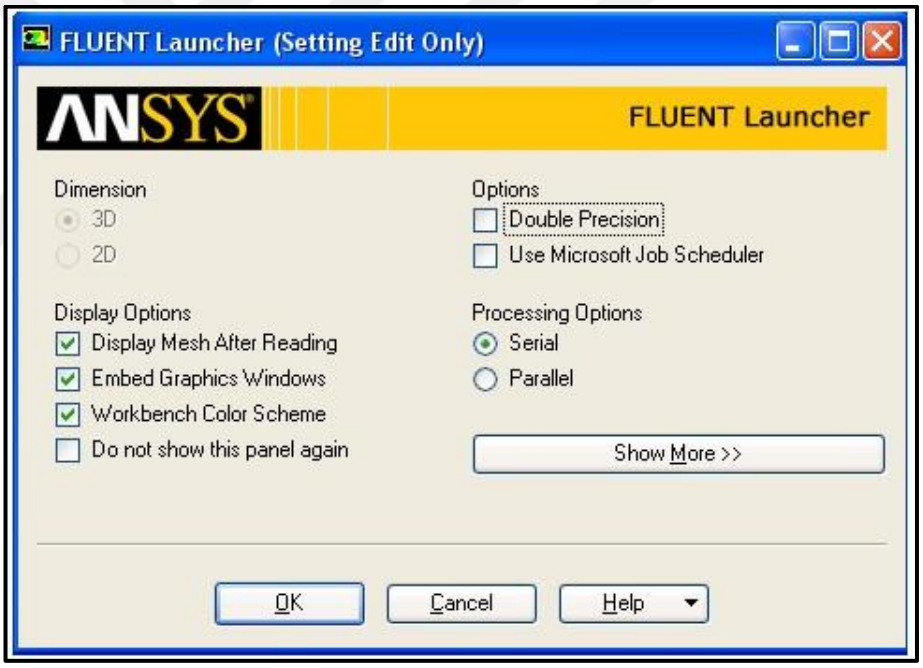

Figure 3.14 Fluent launcher

2. Set general settings for the CFD analysis

When the user chooses the OK selection in start ANSYS Fluent, ANSYS Fluent Application will appear. The follow of water around bridge pier shapes steps must applied to insert all the necessary information in the ANSYS system:

i) Select length in the Quantities list

ii) Select mm in the Units list.

iii) Close the dialog box.

iv) Check the mesh.

v) Specify the water flow direction.

vi) Set up simulation models

The procedure of this work is by select Models code by using turbulent method is the SST k-ω model (Figure 3.15).

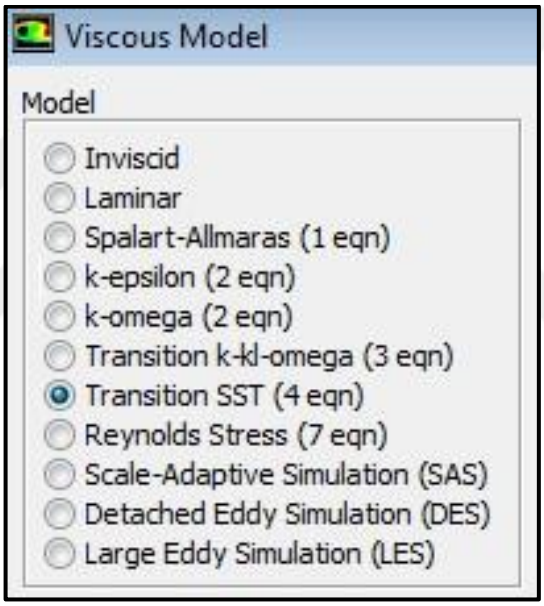

Figure 3.15 Models code

Step 4: Set up the boundary conditions

This step will specify the water velocity

i) Enter x-Velocity

ii) Specify the water flow direction

iii) Specify the water temperature

Step 5: Set up the solution Initialization

The solution configuration task page enables you to specify the values of the flow variables and reset the flow field to these values. The procedure of this work is as in follows:

i) Click solution Initialization (Figure 3.16)
ii) Select standard Initialization
iii) Choose from the code (compute from) the calculation starting
iv) Check from initial values slid all the working values
v) Initializes the data
vi) Run the solver

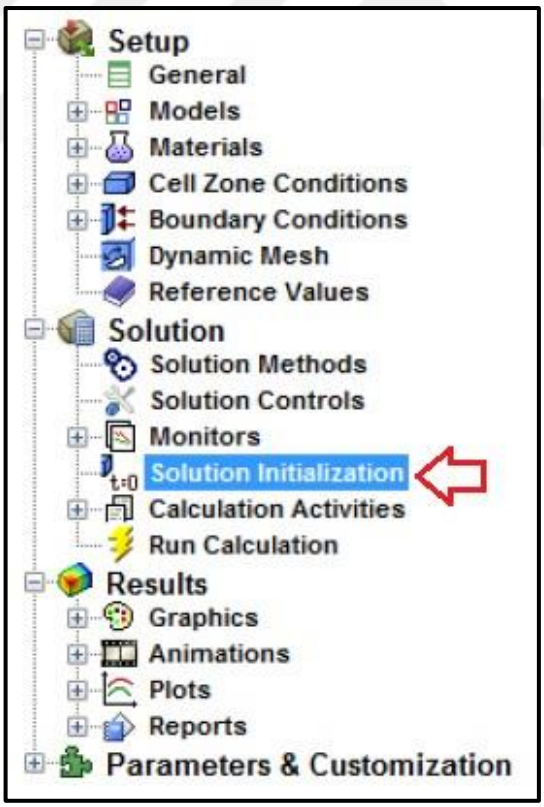

Figure 3.16 ANSYS initial steps

Run the solver is an important process in ANSYS system. It is a powerful tool to describe the water flow behavior. The essential points in this step are the date of working variables, and the number of iteration as shown Figure 3.17.

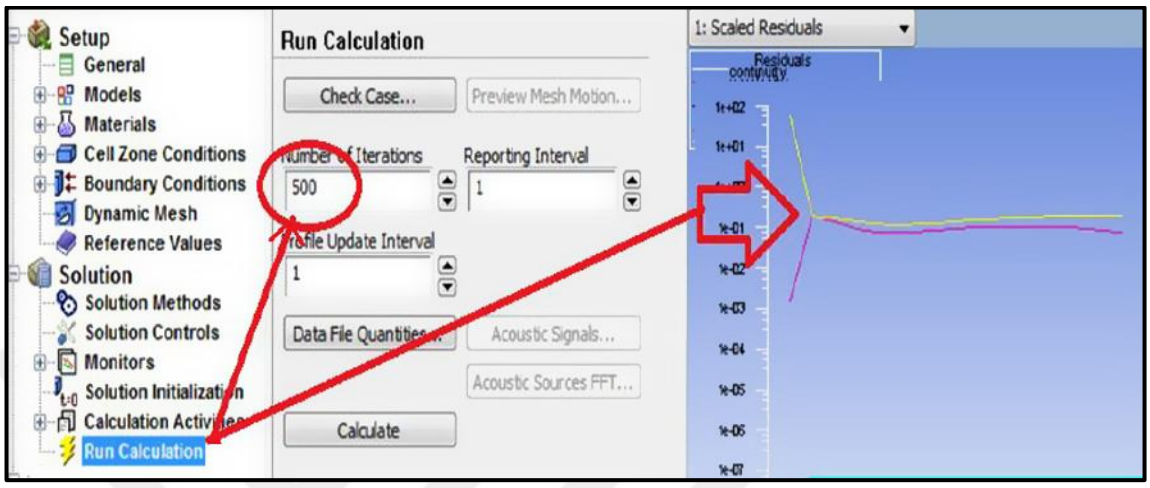

Figure 3.17 Calculate a solution

3.5 Simulation Scenarios

Many scenarios are generated using the water standard. This step is critical as it helps in studying the pressure and speed behavior of various water bridge piers.

For creating scenarios, water kinds must be identified. Three various cases can be used in this study:

1. The first case is to simulate the bridge pier shapes of Formula One Care race.
2. The second case to apply multi-water conditions on the bridge pier shapes.
3. To investigate the water effect on the water flow. The simulation outcomes will register a comparative study of these various kinds of bridge pier shapes.

4. `1RESULTS AND DISCUSSION

The resent chapter will provide the aerodynamics in Bridge pier design. The present study observes different simulation tests of two Bridge piers cases and the third is a suggested pier design to improve the reliability of pier to be used in the bridges projects. It has two primary concerns; the production of lowest pressure to prevent the acting forces on bridge piers caused by the water flow. The tests designed to apply different water velocity values that can reflect the real conditions. ANSYS CFD Fluent software used in run the experiments which contains two groups of scenarios. The experimentations are designed because of two different water velocities. The specific speeds depend on three concerns; the first concern is velocities (0.2, 0.3 and 0.5) meter per second which is used as river water flow speed. All these speeds applied on the brides in Iraq subjected on Degla river, Baghdad Iraq named the Iron Bridge and Al-Muadam Bridge. The results of the CFD simulation for the three kinds of pier analyzed the properties of the water flow and evaluated the pressure applied to it based on different levels in (x, y and z) directions and directed the scholar to the optimal outcomes for comparison. Current outcomes achieve the purpose of this study and provide a brief discussion based on four sections. The first section presents the aerodynamic analysis of the iron bridge by means of ANSYS outcomes and plotting the numerical outcomes. The second division offers the aerodynamic analysis of Al-Muadam Bridge. At the end an optimization presented with a comparison.

4.1 Flow Around the Bridge Piers Plane

Current study, resulted data were obtained on the horizontal planes of the bridge piers. The various symbols associated with the arrangement of the bridge pier, used in this thesis, are revealed in the Figure 4.1. In this figure, the X and Y axes are represented along the current-wise direction and the transverse direction, correspondingly; whereas D is the equivalent diameter**.**

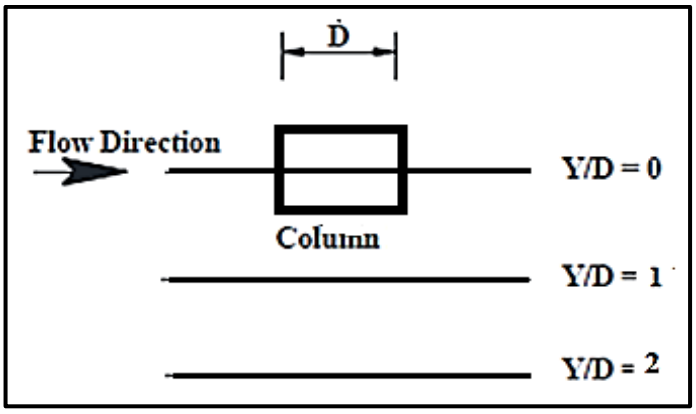

Figure 4.1 Diagram drawing of various axis of resulted data analysis in horizontal planes

The outcomes on the field of flow and turbulence features of the flow around bridge piers and the influence of spacing among columns are offered in the succeeding sections.

4.2 ANSYS Evaluation of the Iron Bridge (Case 1)

The pier is the most crucial component in the bridge. For that, this study aims to investigate the aerodynamic characteristic in bridge pier. The flow characteristic can be recognized by observing the water flow behavior in different types of piers and water velocity. Different shape of the bridge piers produces different flow behavior around the two sides of the bridge pier. This generates a compression change founded on a physical rule identified as the Bernoulli principle. As this compression attempts to equilibrate, the water flow tends to move in the direction of low compression. In order to characterize the aerodynamic forces acting on the bridge pier. The present study observes the aerodynamic behavior around the bridge pier by using CFD.

ANSYS role of CFD in design changes rely on the phase of the study. Computational fluid dynamics are used in the shape of a two-dimensional, structured lattice flow solver with mutually Euler and Reynolds mean Navier-Stokes equations. The numerical model is prepared and run with CAD software that creates boundary conditions for the analysis. This analysis outcomes act a significant part in optimizing the design

mechanisms so that there is slightest pressure on the pier surface and swirl of water flow.

4.2.1 Iron bridge flow pattern

The vector diagrams and flow line diagrams as revealed in Figure 4.2 for the case of a single column obviously represent the flow patterns around the bridge pier. ANSYS simulates the chosen cases by defining them according to boundary conditions. Five basic properties used in the CFD-ANSYS simulation process are shown in Table 4.1. Various scenarios are produced using the pressure and velocity behavior of different bridge piers subjected to water motion.

Table 4.1 Operating parameters

	Parameter	**Input value**
1	Water flow speed	0.2, 0.3, 0.5 mps
2	Operating temperature	288.16 K
3	Density	1016 Kg/m3
4	Model	SST k-ω
5	Fluid	Water

The flow characteristic can be recognized by observing the water flow behavior in different types of piers. The effect of pressure variation on the bridge pier indicate the differences. The water flow speed is crucial because it control the effect of water movement which changes the surface pressure on piers (Figure 4.2).

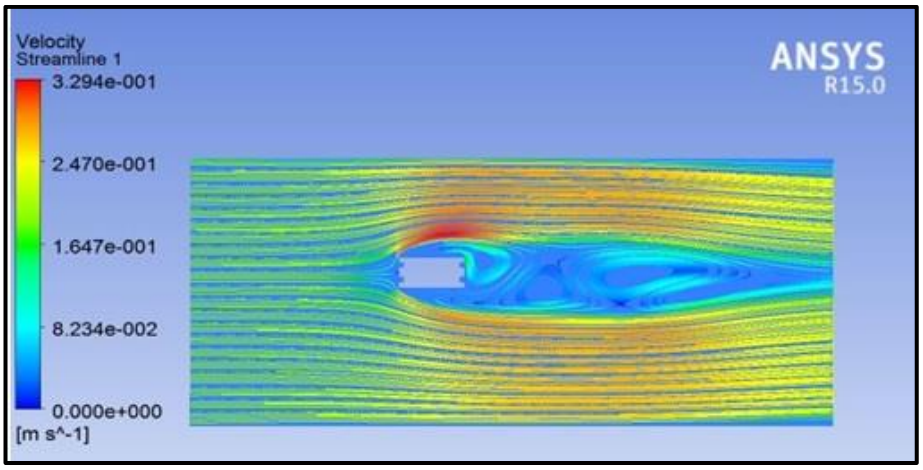

Velocity Flow Pattern of 0.2 mps

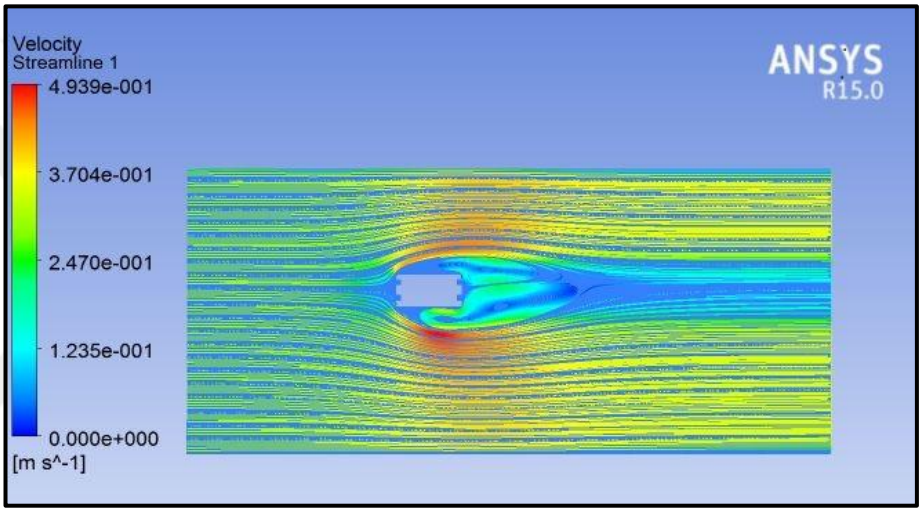

Velocity Flow Pattern of 0.3 mps

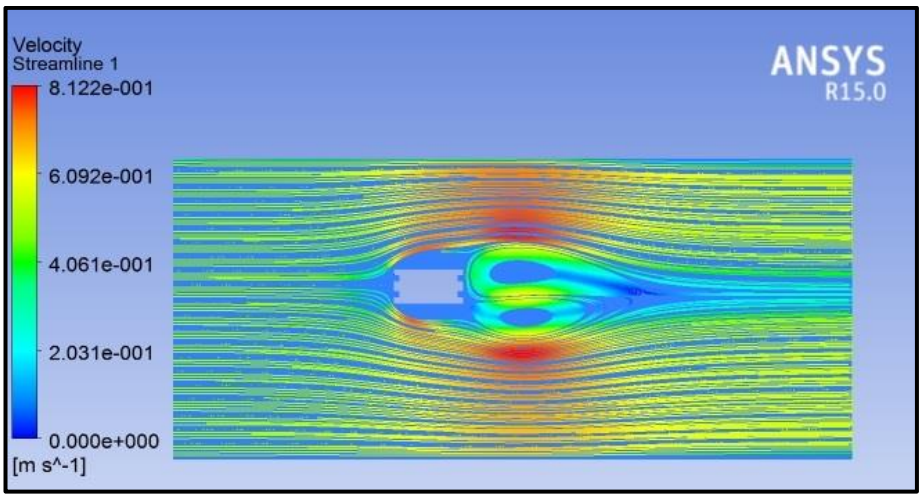

Velocity Flow Pattern of 0.5 mps

Figure 4.2 Velocity flow pattern of the iron bridge simulation results

It is observed that the maximum pressure affect in the tip of the bridge pier as shown in the red color of the pressure profile. This observation approved that there is a high down force in this point, the affected force component will have applied perpendicularly on the longitudinal axis of the bridge pier section. But with the increase of water velocity, the vortex appears as shown in Figure 4.3 in the velocity profile. The vortex will increase the drag force which cause several aerodynamic problems.

Due to boundary layer separation at the vacuum side of the bridge pier stationed below the critical edge vortex which broke down that resulted in loss of pressure. It is seen that the water characteristics have been changed by the changes of water velocity; therefore, the speed profiles observe an rise in water velocity at the side of the bridge pier surfaces and a reduction in the upper surface as specified by the red region. In current study, the force will increase because there is an inverse relationship between the force and the water speed (Figure 4.4).

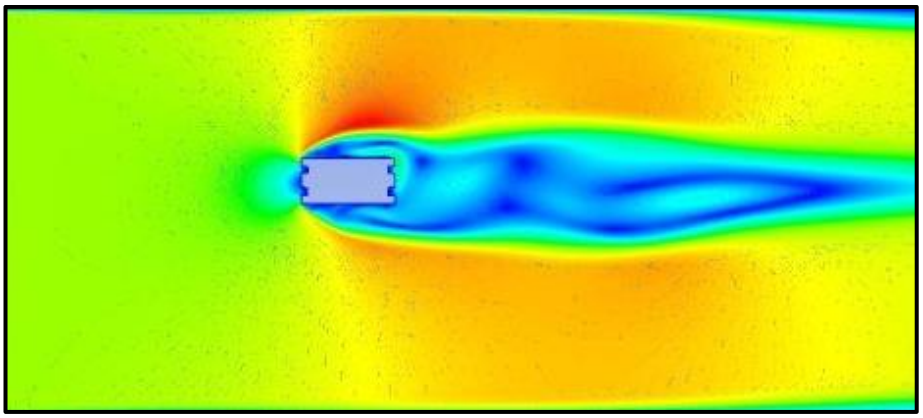

Velocity Flow Pattern of 0.2 mps

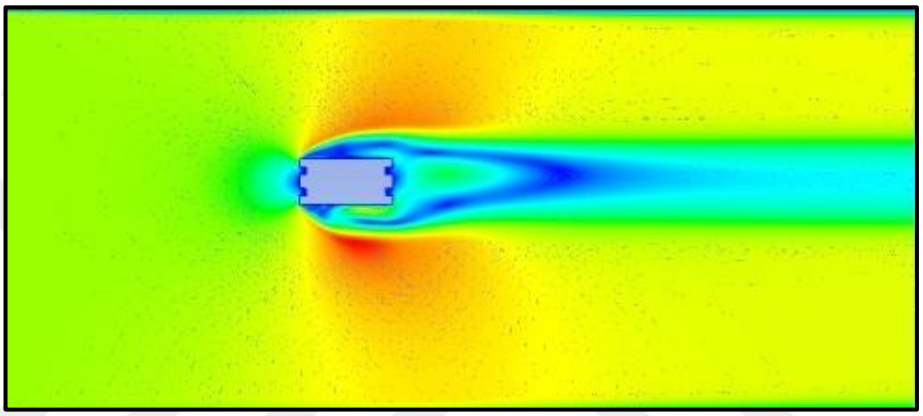

Velocity Flow Pattern of 0.3 mps

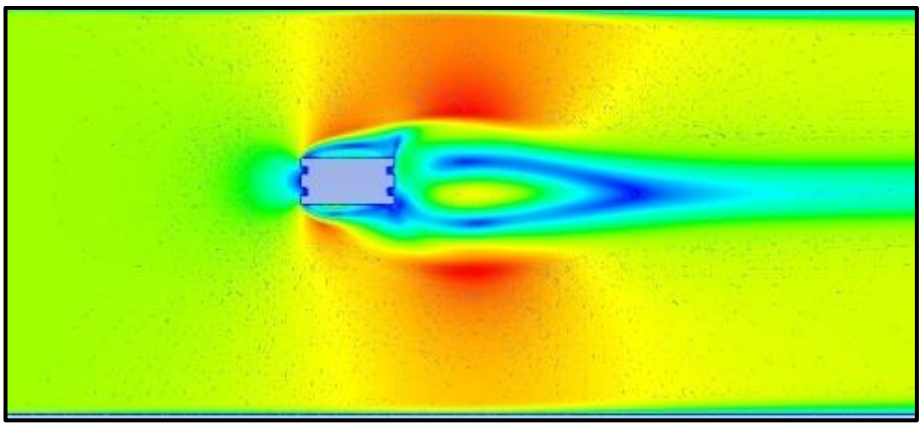

Velocity Flow Pattern of 0.5 mps

Figure 4.3 Velocity profile of the iron bridge simulation results

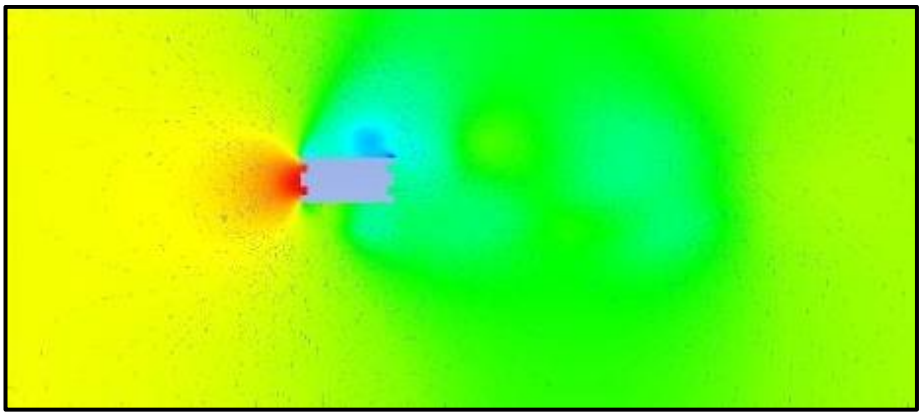

Pressure Pattern of 0.2 mps

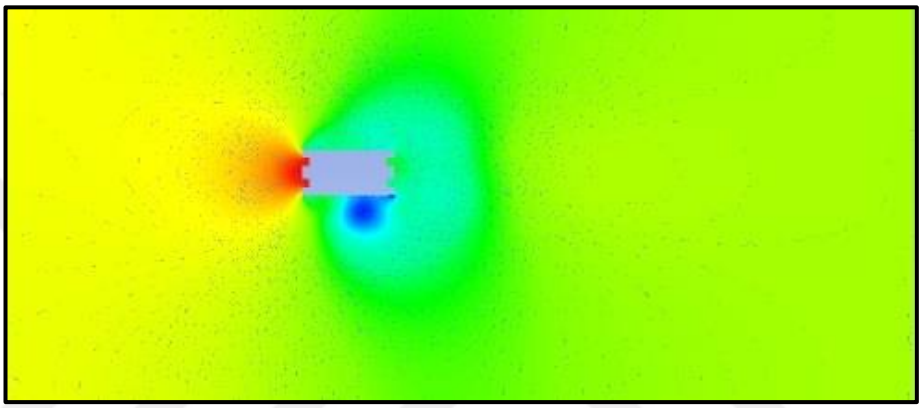

Pressure Pattern of 0.3 mps

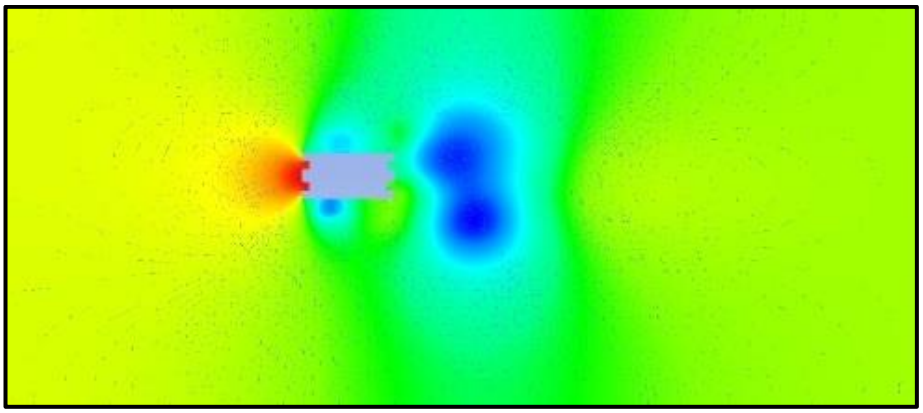

Pressure Pattern of 0.5 mps

Figure 4.4 Pressure profile of the iron bridge simulation results

Pressure lines notice an rise in the front surface of the bridge pier and a reduction in the rear surface. This outcome specifies that the resistance against the direction of flow will create a negative force which means that the force will increase because there is a

positive relationship between the force and the water pressure in the bridge pier surfaces.

4.2.2 Velocity numerical results of the iron bridge case 1

The numerical results which obtained by the ANSYS -FLUNT processes present a set of values. These values represent the changes results of the velocity based on the changes in distances far away from the center of column. Figure 4.5 shows the distribution of water velocity distribution alongside three diverse longitudinal axes Y/D = 0, 1 and 2. Plans show pockets of greater and lesser speed values at the side and heels of the shaft, in that order. The rise velocity value on the column side is due to the blockage due to the presence of the column which reduced the flow. It is seen from the results that the velocity increases incrementally with the increasing of the Y/D. This fact can be observed clearly by plotting the results. Figure 4.6 to Figure 4.7 shows the relationship of the bridge pier down force effect due to the shape effect.

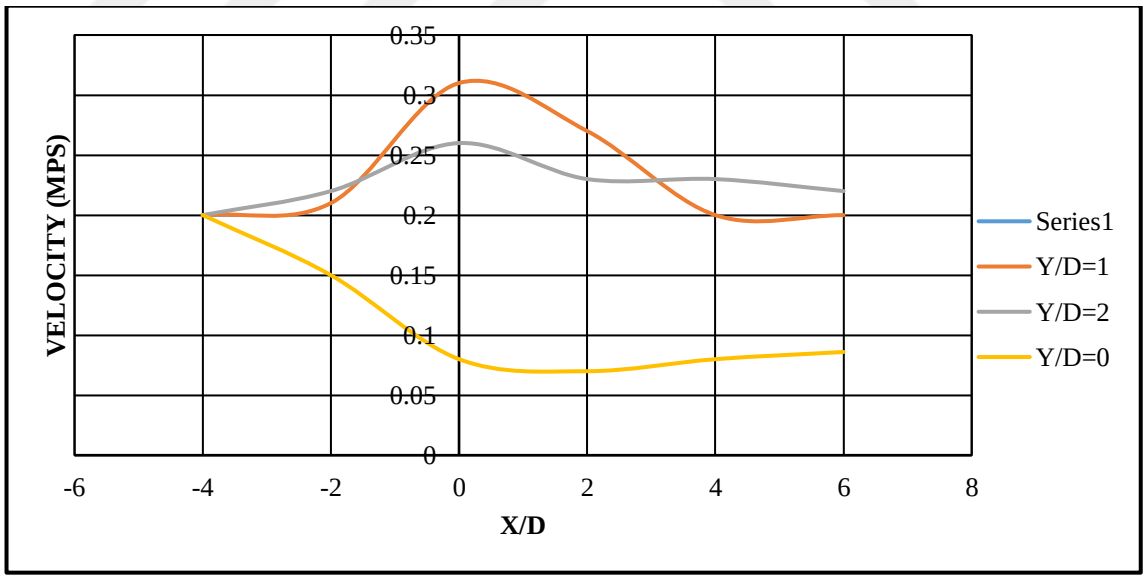

Figure 4.5 Cutting profile for single column case speed component of iron bridge, vel. 0.2 m/s

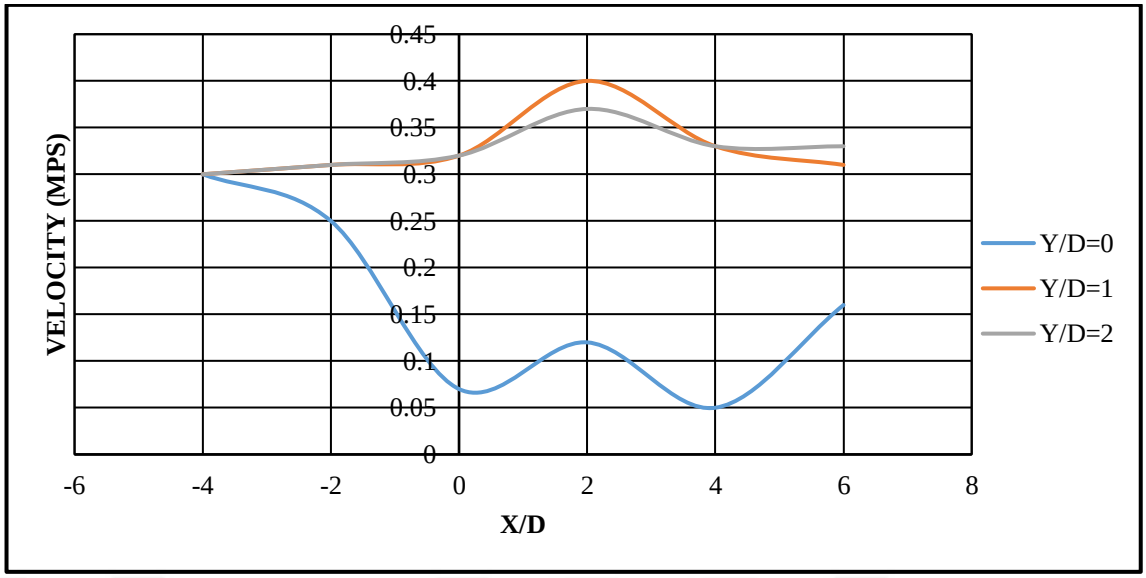

Figure 4.6 Cutting profile for single column case speed component of iron bridge, vel. 0.3 m/s

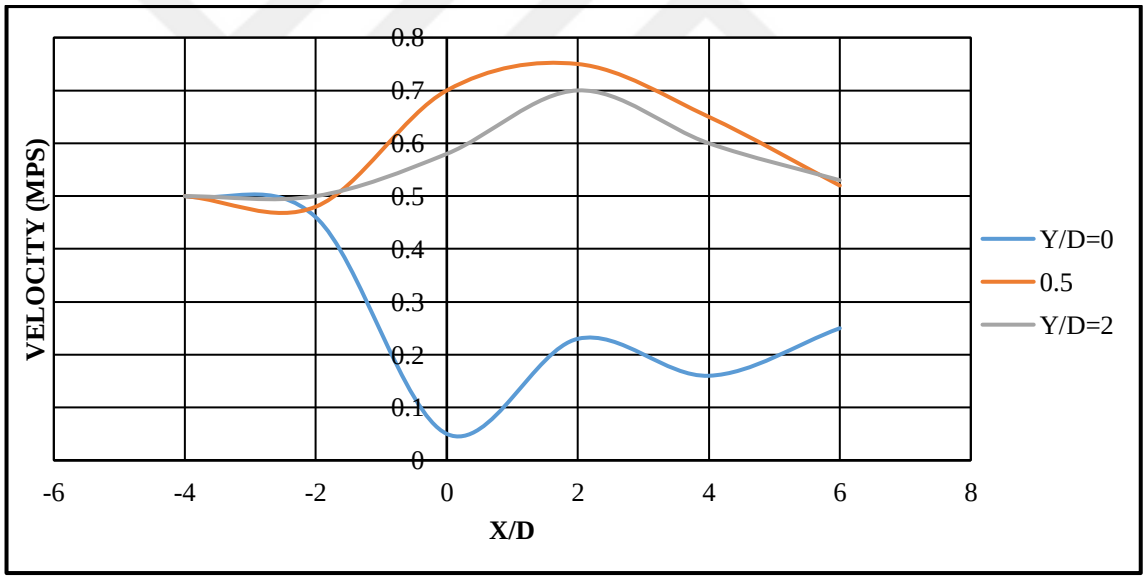

Figure 4.7 Cutting profile for single column case speed component of iron bridge, vel. 0.5 m/s

4.2.3 Pressure numerical results of the iron bridge case 1

Investigation of Aerodynamic characteristics achieved by running the ANSYS solver based on first case of bridge pier shape. It is detected that the compression distribution around the pier is convergent in both sides of the pier (Figure 4.8). The maximum

pressure affect in the tip of the pier, this notification approves that the shape of the tip is an important issue, and the affected force component couldn't have applied perpendicularly on the longitudinal axis of the pier section (Figure 4.9, Figure 4.10).

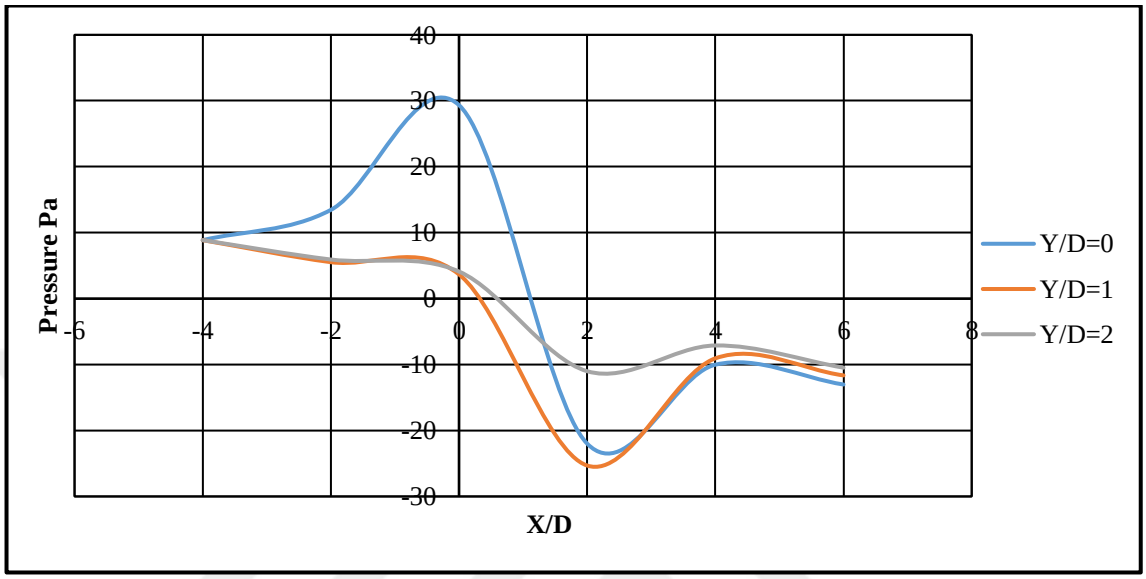

Figure 4.8 Cutting profile of compression component for single column case of iron bridge, vel. 0.2 m/s

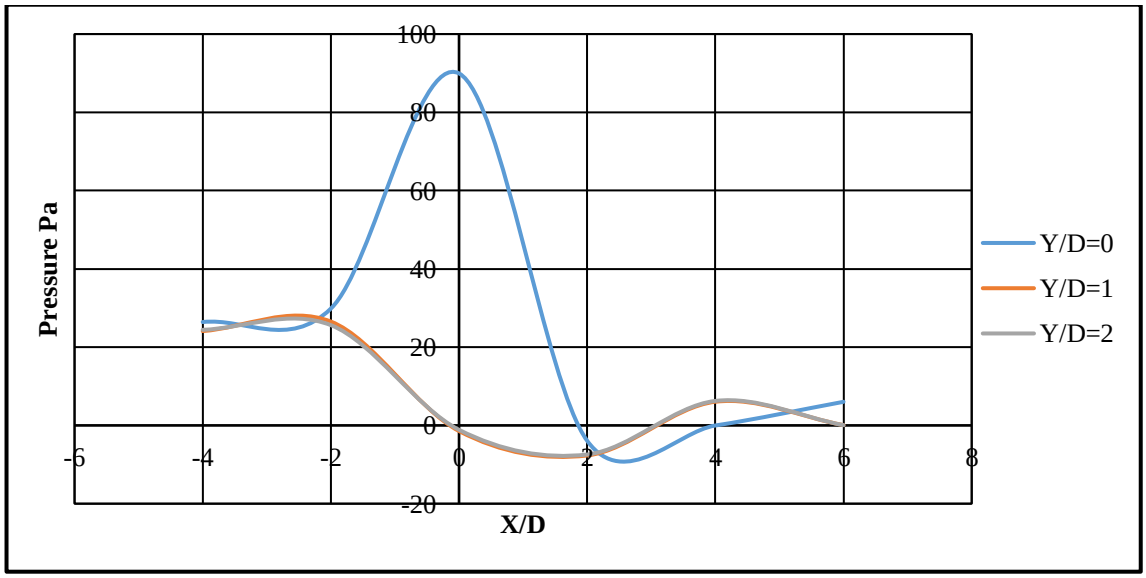

Figure 4.9 Cutting profile of compression component for single column case of iron bridge, vel. 0.3 m/s

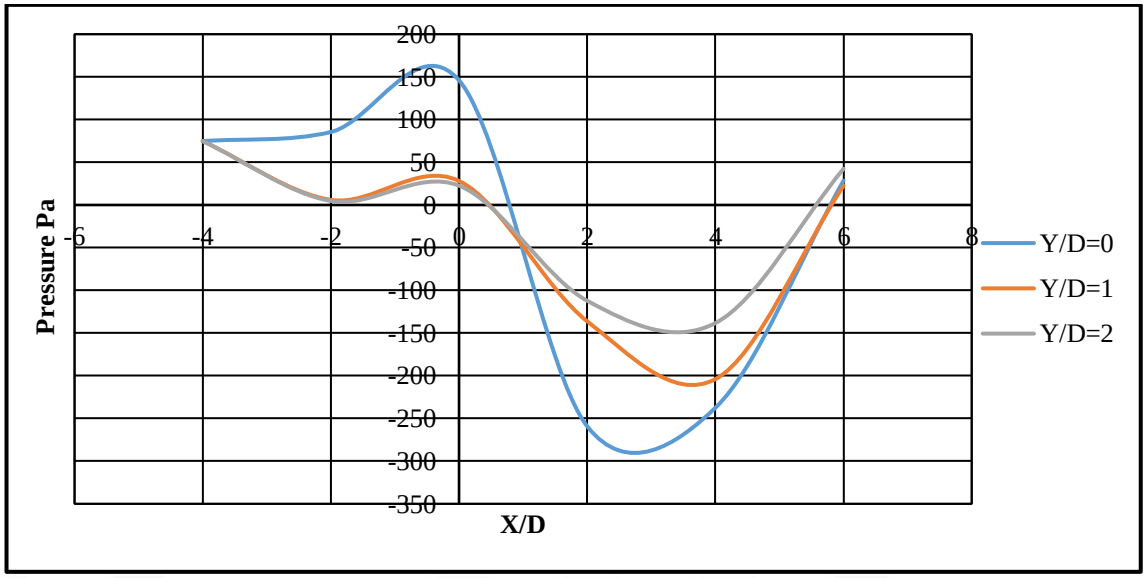

Figure 4.10 Cutting profile of compression component for single column case of iron bridge, vel. 0.5 mps

4.3 ANSYS Evaluation of Al-Muadam Bridge (Case 2)

The present case observes the aerodynamic behavior around rectangular bridge pier by using CFD ANSYS. The numerical model is also prepared and run with CAD software that creates boundary conditions for the analysis. This analysis outcome acts an important part in optimizing design components so that there is minimal pressure on the pier surface and swirl of water flow.

4.3.1 Al-muadam bridge flow pattern

The vector and steam line diagrams presented in Figure 4.11 for the case of a single column obviously show the flow patterns around the rectangular bridge pier. ANSYS simulates the selected cases by defining them according to boundary conditions. There are five basic characteristics used in the CFD-ANSYS simulation procedure that are the same as in the first case flow characteristic can be recognized by observing the water flow behavior in this type of piers. The influence of pressure variation on the bridge pier indicates the differences. The water flow speed is crucial because it control the effect of water movement which changes the surface pressure on piers.

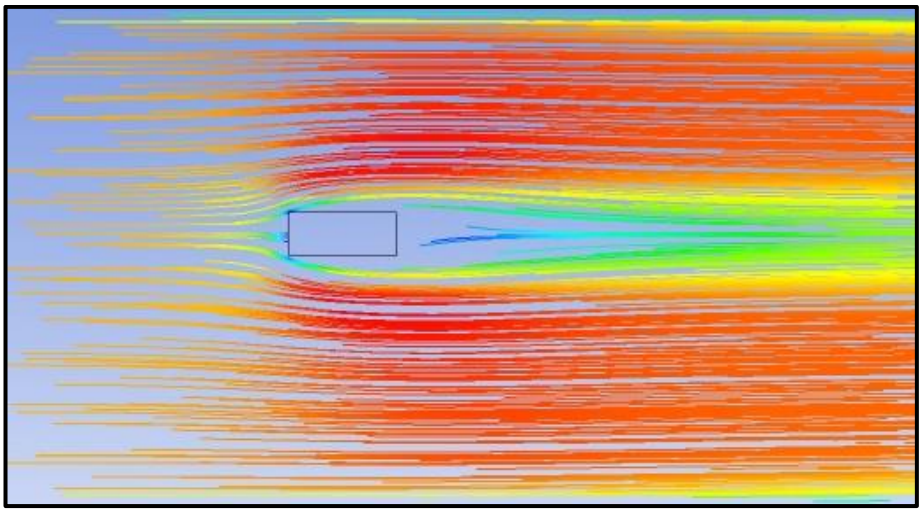

Velocity Flow Pattern of 0.2 mps

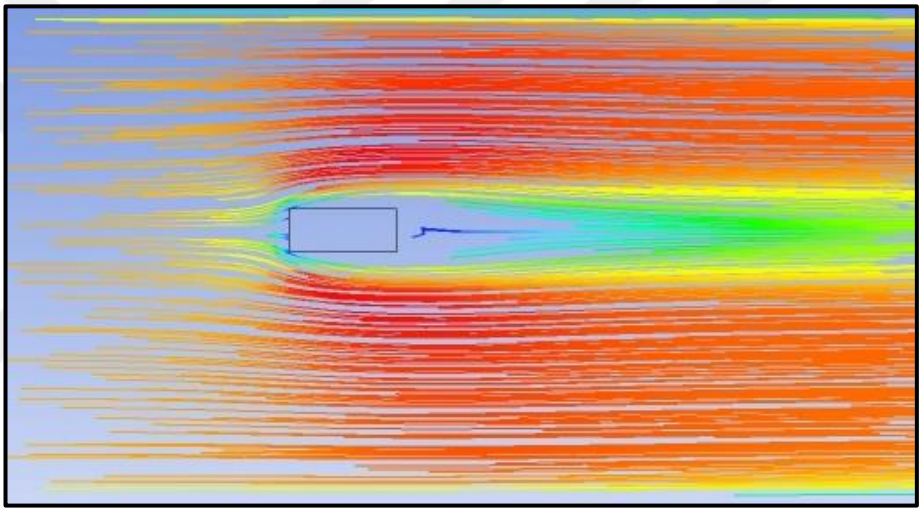

Velocity Flow Pattern of 0.3 mps

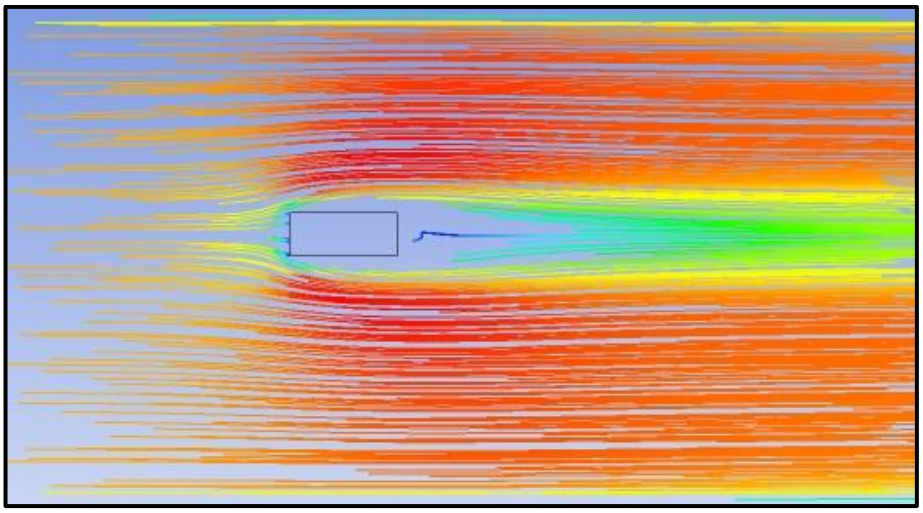

Velocity Flow Pattern of 0.5 mps

Figure 4.11 Velocity flow pattern of the Al-Muadam bridge simulation results

It is observed that the maximum pressure affect in the tip of the bridge pier as shown in the red color of the pressure profile. This observation approved that there is a high down force in this point, the affected force component will have applied perpendicularly on the longitudinal axis of the bridge pier section. But with the increase of water velocity, the vortex appears as shown in Figure 4.12 in the velocity profile. The vortex will increase the drag force which cause several aerodynamic problems.

Due to boundary layer separation at the suction side of the bridge pier stationed below the critical edge vortex which broke down that resulted in loss of pressure. It is seen that the water characteristics have been changed by the changes of water velocity; therefore, the speed profiles note a rise in water velocity at the side of the bridge pier surfaces and a reduction in the upper surface as presented in the red area. In this case, the force will increase because there is an inverse relationship between the force and the water speed (Figure 4.11).

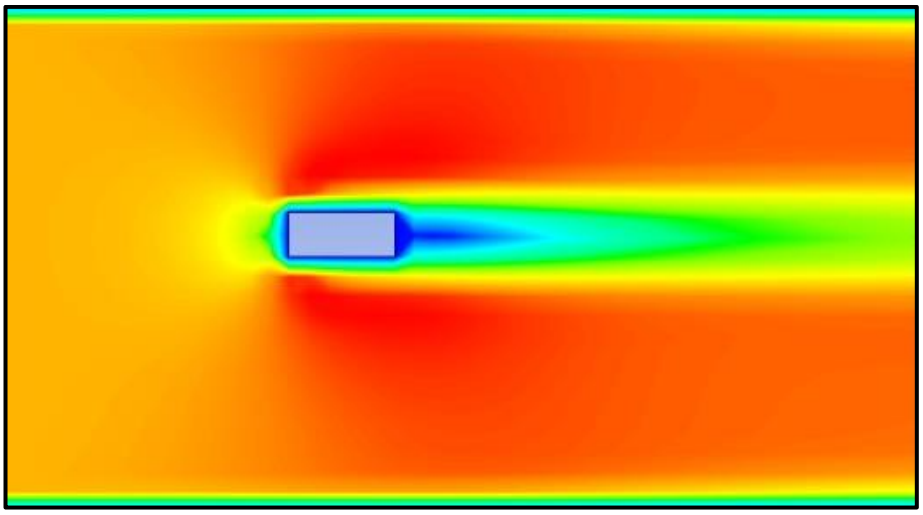

Velocity Flow Pattern of 0.2 mps

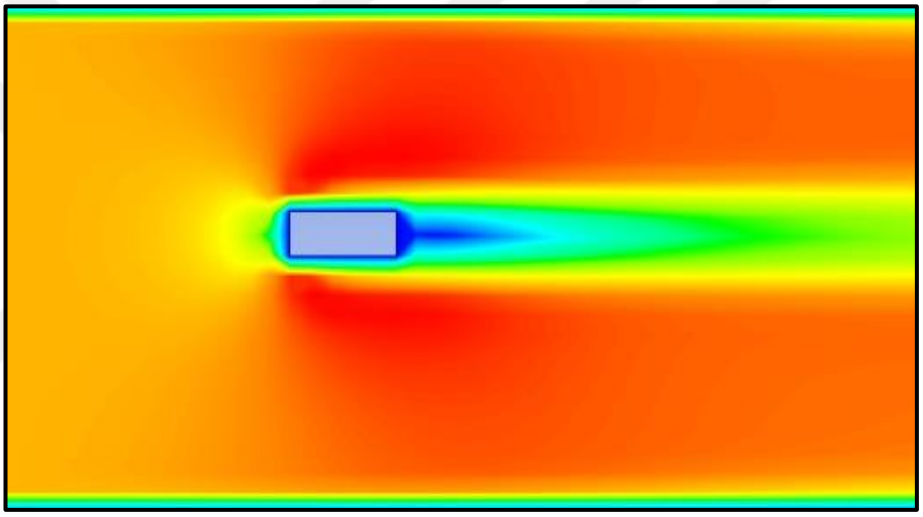

Velocity Flow Pattern of 0.3 mps

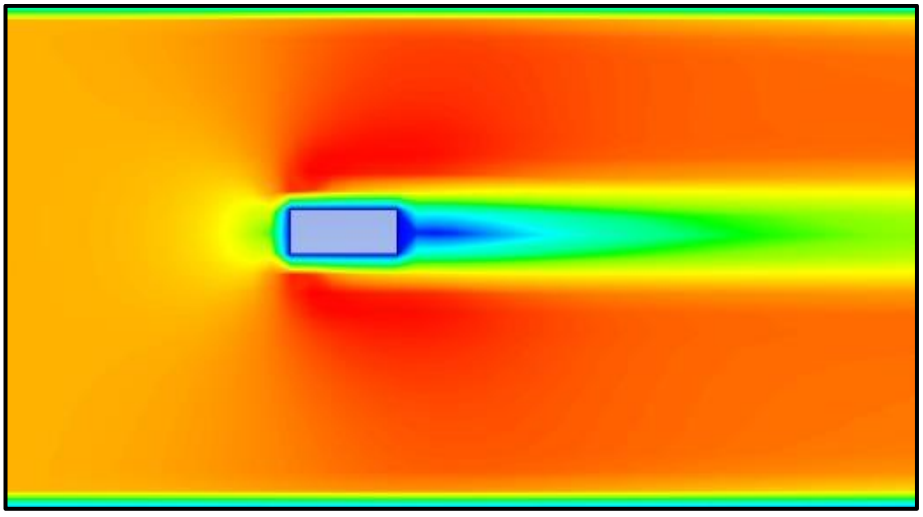

Velocity Flow Pattern of 0.5 mps

Figure 4.12 Velocity profile of Al-Muadam bridge simulation results

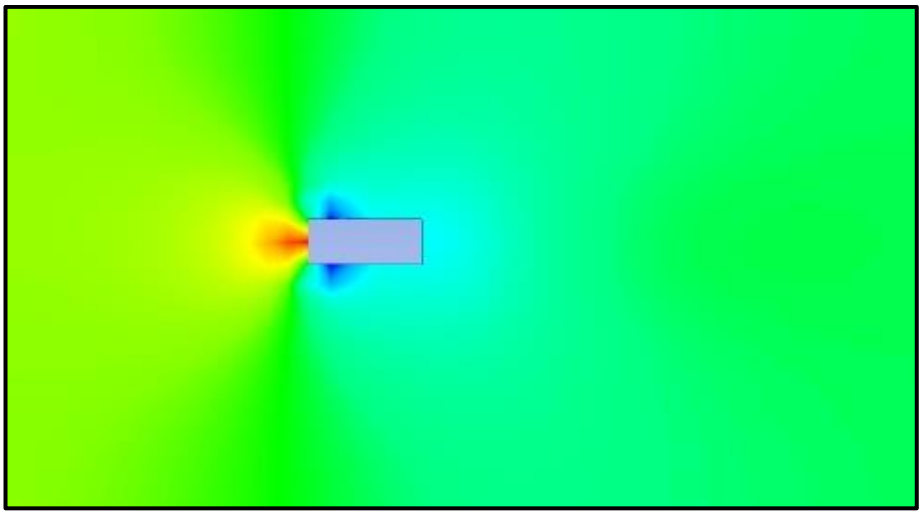

Pressure Pattern of 0.2 mps

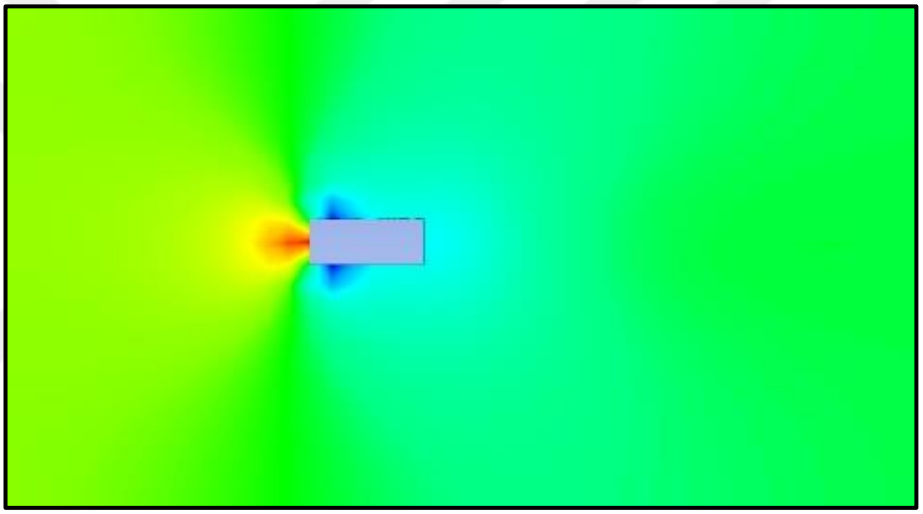

Pressure Pattern of 0.3 mps

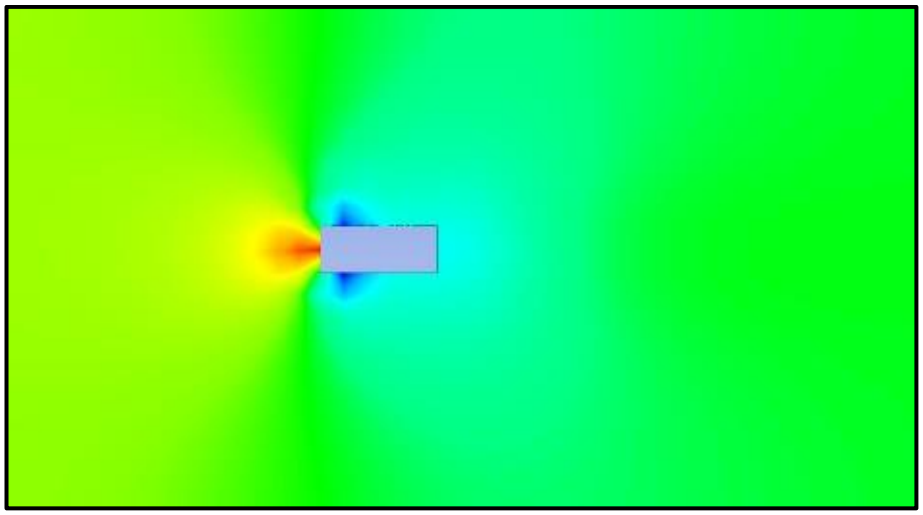

Pressure Pattern of 0.5 mps

Figure 4.13 Pressure profile of Al-Muadam bridge simulation results

The pressure contours observe a rise in the front surface of the bridge pier and reduction in the back surface. This result indicates that the resistance against the flow course will create a negative force which means that the force will increase because there is a positive relationship between the force and the water pressure in the bridge pier surfaces (Figure 4.13).

4.3.2 Velocity numerical results of Al-Muadam bridge case 2

The numerical results which obtained by the ANSYS -FLUNT processes present a set of values. These values represent the changes results of the velocity based on the changes in distances far away from the center of column. Figure 4.14 shows the distribution of water velocity along three diverse longitudinal axes Y/D = 0, 1 and 2. Contour diagrams demonstrate pockets with greater and lesser velocity values on the side and heel of the column. The rise of speed value located at the side of the column is due to the obstacle because of the presence of column causing in flow contraction. It is seen from the results that the velocity increases incrementally with the increasing of the Y/D. This fact can be observed clearly by plotting the results. Figure 4.15 and Figure 4.16 shows the relationship of the bridge pier down force effect due to the shape effect.

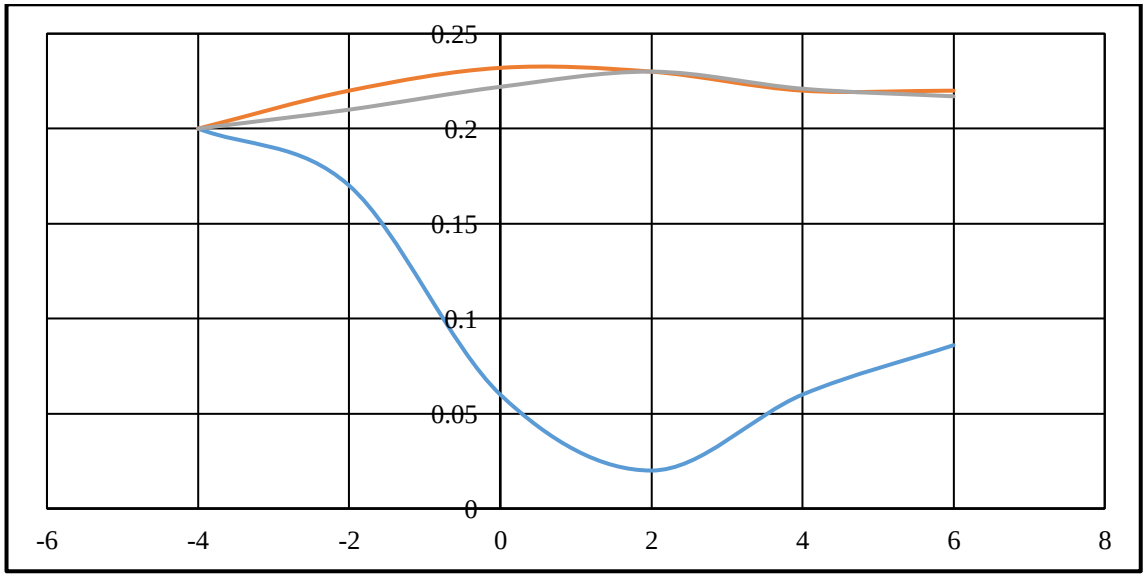

Figure 4.14 Cutting profile for ducting velocity component for one column case of Al-Muadam bridge, vel. 0.2 m/s

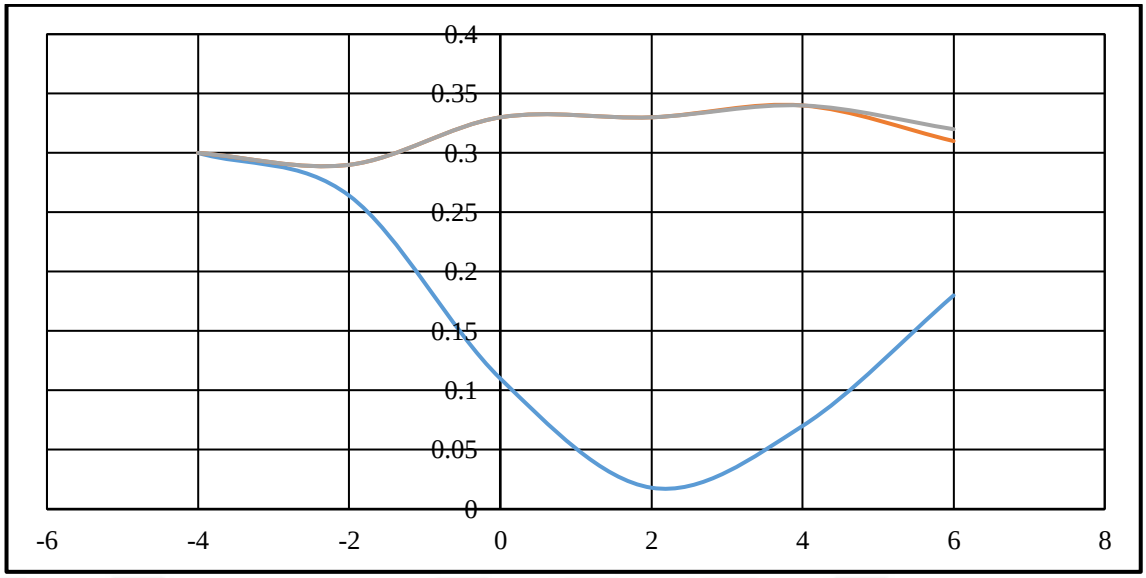

Figure 4.15 Cutting profile for ducting velocity component for one column case of Al-Muadam bridge, vel. 0.3 m/s

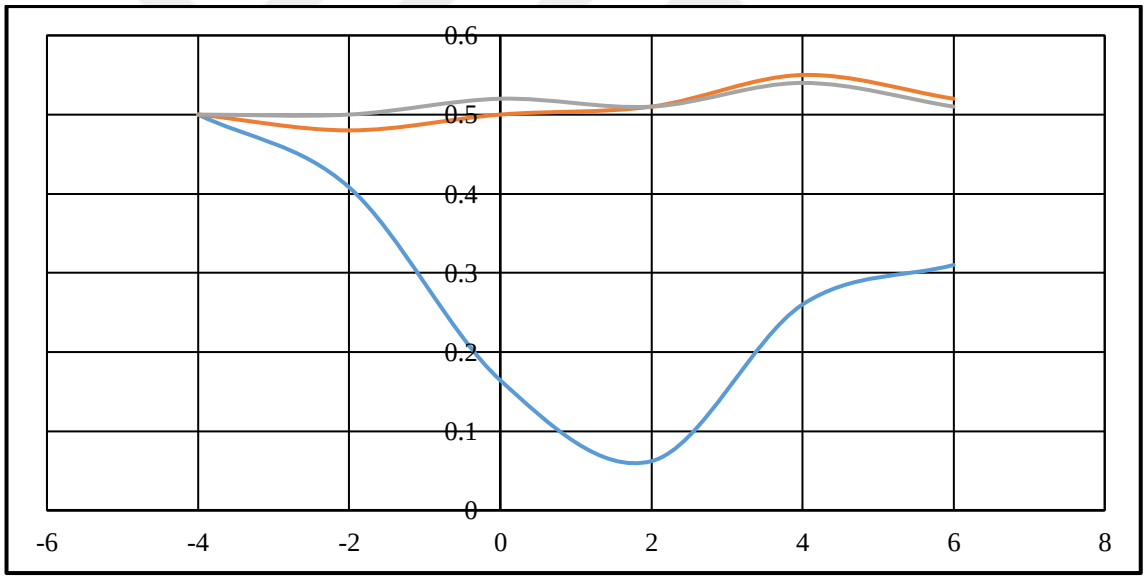

Figure 4.16 Cutting profile for ducting velocity component for one column case of Al-Muadam bridge, vel. 0.5 m/s

4.3.3 Pressure numerical results of al-muadam bridge case 2

Investigation of Aerodynamic characteristics achieved by running the ANSYS solver based on first case of bridge pier shape. It is detected that the compression distribution around the pier is convergent in both sides of the pier (Figure 4.17). The maximum

pressure affect in the tip of the pier, this notification approves that the shape of the tip is an important issue, and the affected force component couldn't apply perpendicularly on the longitudinal axis of the pier section (Figure 4.18, Figure 4.19).

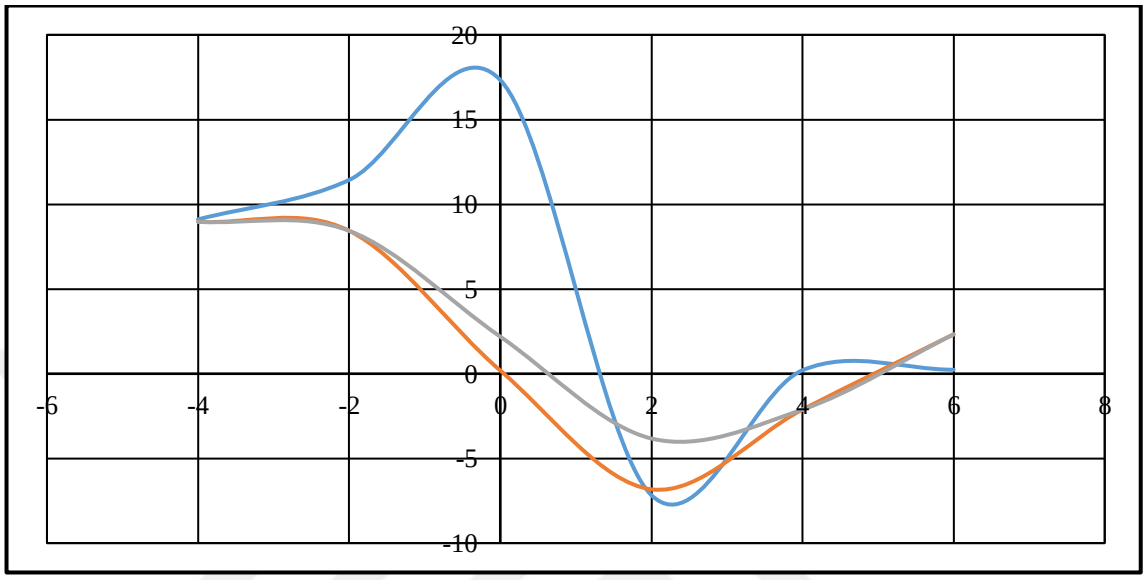

Figure 4.17 Cutting profile for compression component for one column case of Al-Muadam bridge vel. 0.2 m/s

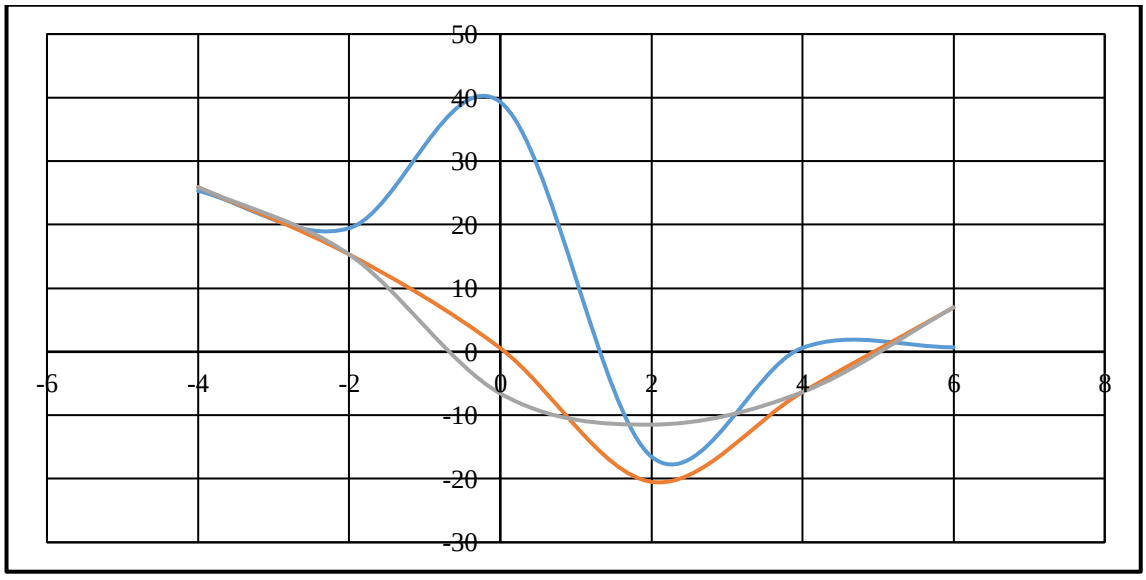

Figure 4.18 Cutting profile for compression component for one column case of Al-Muadam bridge, vel. 0.3 m/s

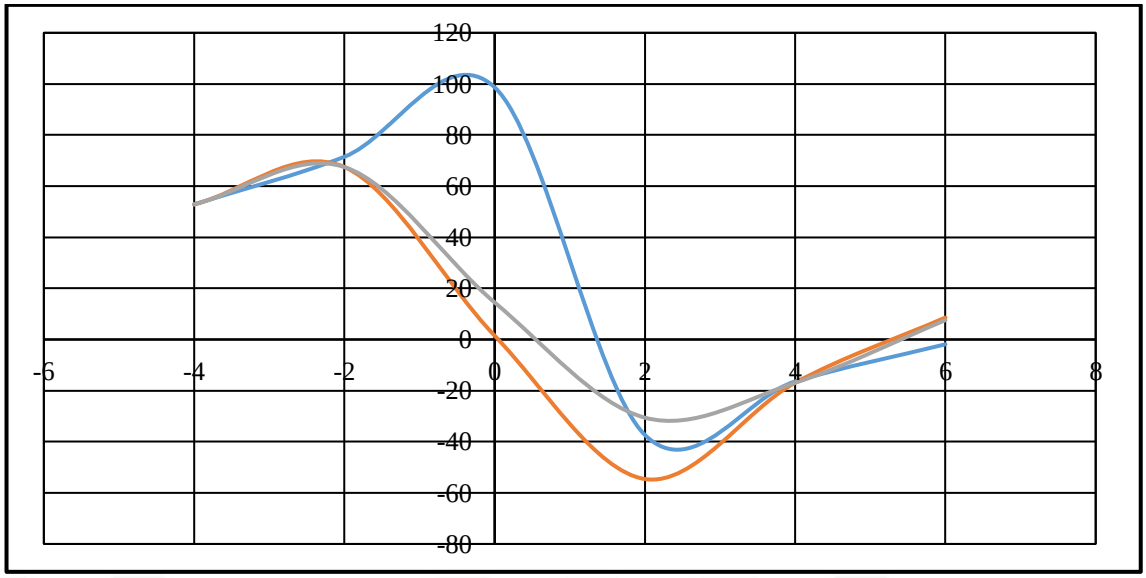

Figure 4.19 Cutting profile for compression component for one column case of Al-Muadam bridge, vel. 0.5 m/s

4.4 Optimization of Pier Front Face

Based on the present cases, the researcher develops a new front pier shape using circular shape. The finding of optimal pier founded on the existing simulations in earlier mentioned sections. Understanding the water flow behavior was useful to develop the front pier in order to get better understanding for pressure effect. Using front pier design provides unique results. Figure 4.20 shows the new suggestion design of the optimized pier.

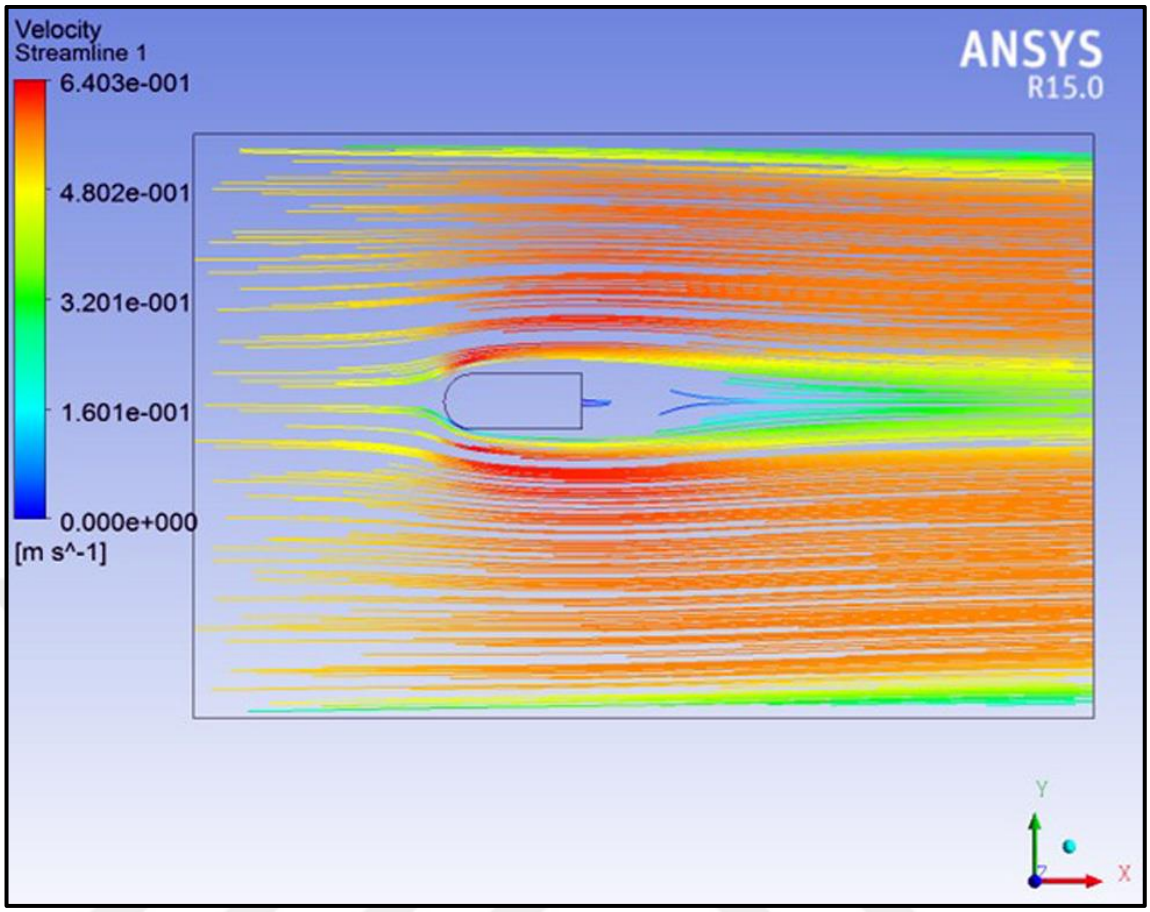

Figure 4.20 The new suggested front pier design (Velocity, 5 mps)

This suggested design gives a narrow front area to create minimum pressure load. And the curve in front of pier will provide less vortex effect. The researcher found from the presented work that there is an optimal shape of pier which can provide the best water flow as show in Figures (Figure 4.21, Figure 4.22, Figure 4.23).

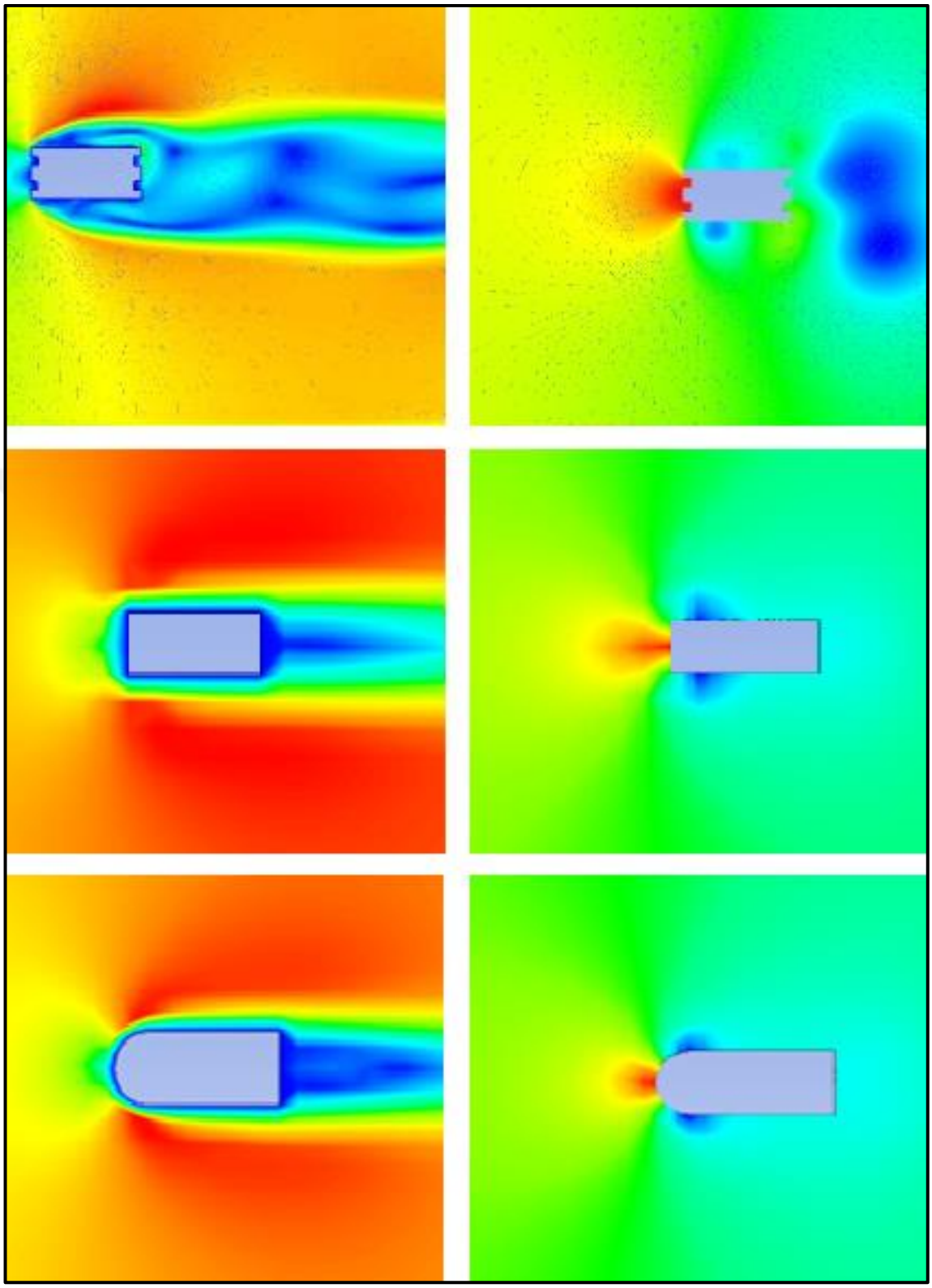

Figure 4.21 Comparison of pressure and water flow effect of Pier design

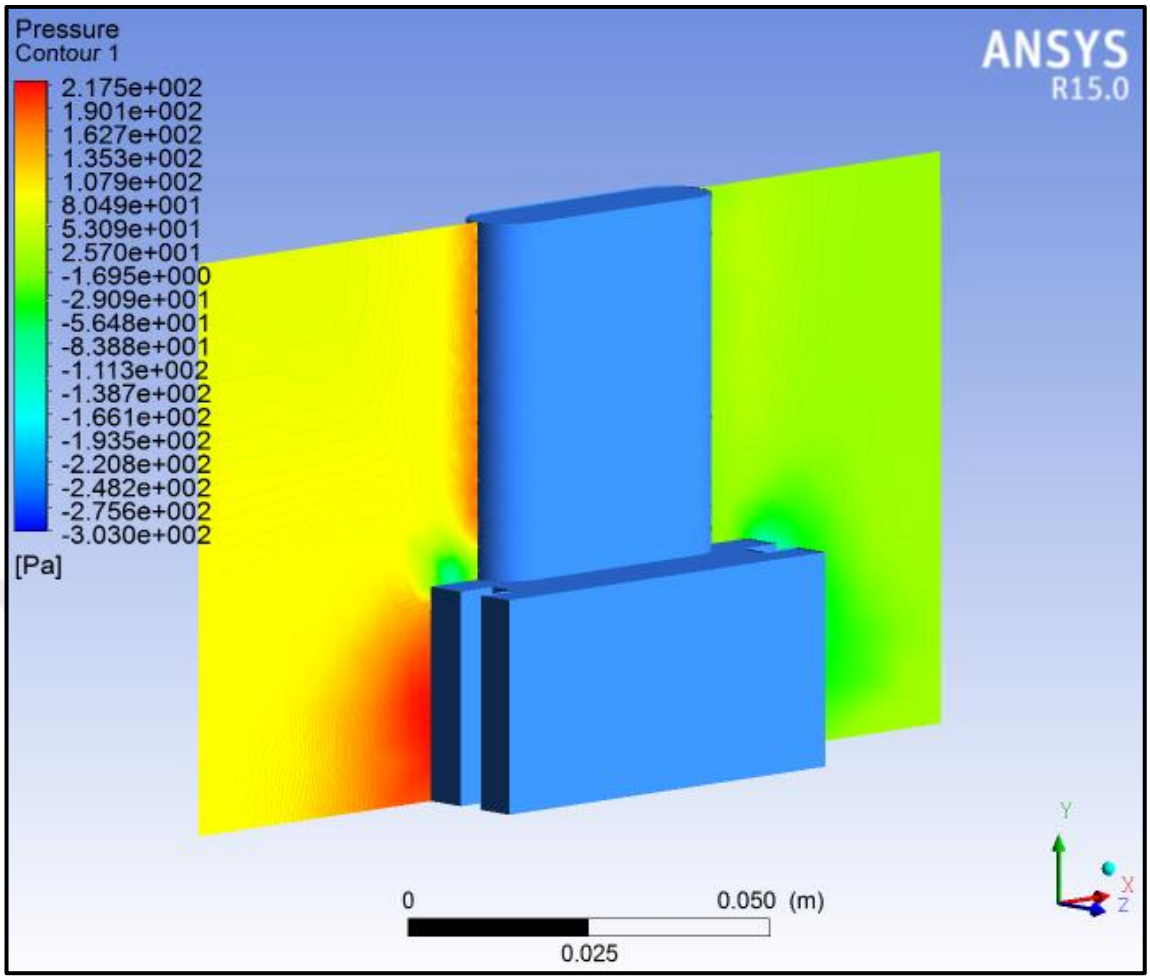

Figure 4.22 Pressure effect of 3D simulation results (Case 1)

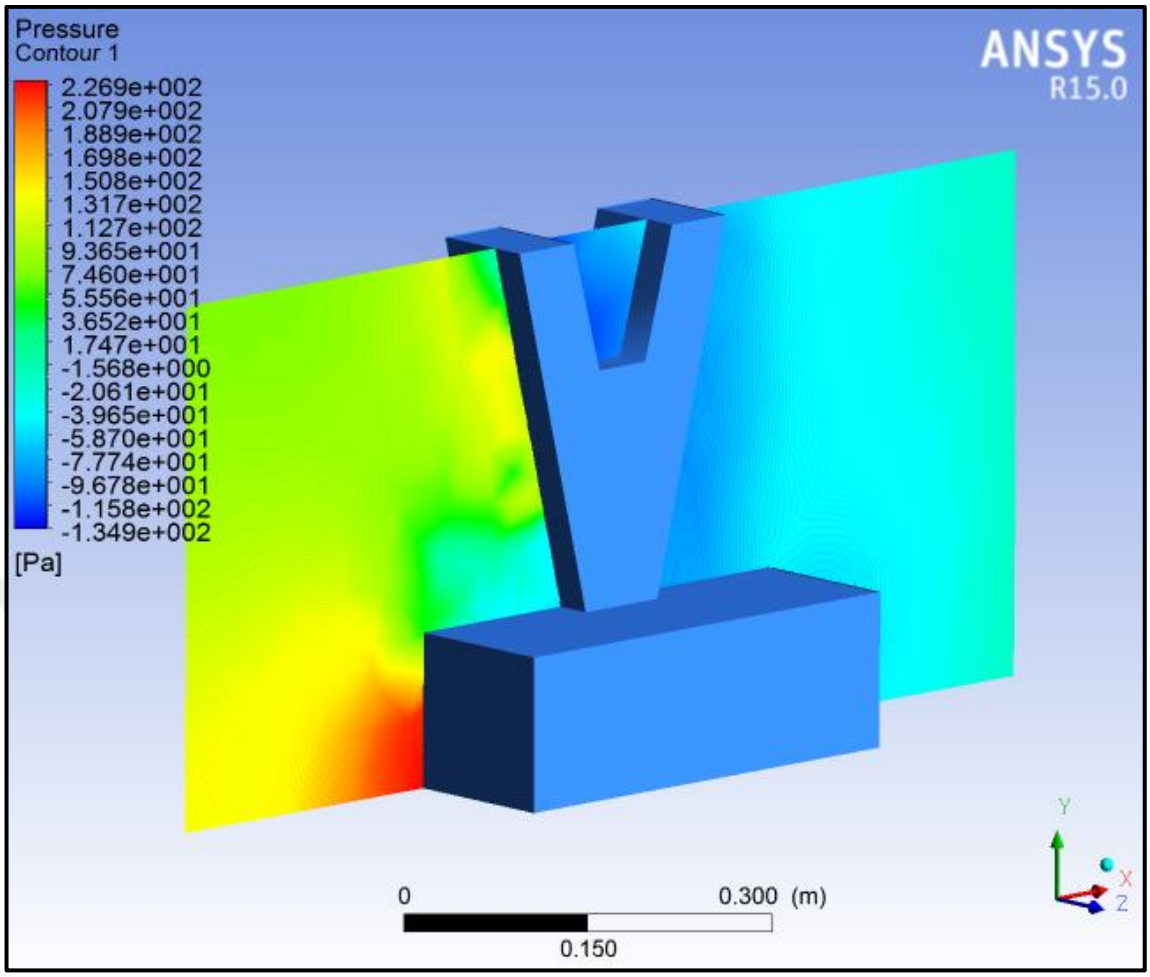

Figure 4.23 Pressure effect of 3D simulation results (Case 2)

From the 3D pressure results, it noticeable that the most compression is effect on the pier base.

5. CONCLUSION AND RECOMMENDATION

This chapter presents the conclusion and recommendation of the present work. The methodology of this chapter addressed the research gaps and achieved the objectives of this study. Two contributions were achieved in this study, the first one is the analysis of two types of piers. They are Al-Muadam Bridge and the Iron Bridge. The analysis was done based on the velocity and pressure effect on multi-levels of water surfaces. The second is the optimization of the pier design by adding a specific curve in the head of the pier. This result was obtained after finding the better design of selected piers. The advanced technology applied in the present work is the CFD ANSYS program. The simulation method in this thesis provides a better value of the pressure distribution.

5.1 Conclusions

The CFD simulation results observe different turbulence models. The study observes that the pier design has a major effect on pressure distribution. In order to investigate the complex pier correlations, the forces are considered as a complex dependence of the shape, flow conditions, and also inclinations. The study observes that the optimal pressure distribution effect is concerned with the front curve which minimizes pressure load and reduces the vortex behind the pier. Based on these facts, the results of the piers test results summarized in the pier

i) The CFD ANSYS results of the Al-Muadam Bridge observed which the pressure force increases incrementally on the pier. This result observes the importance of the surface shape of the pier to generate the pressure force based on Y/L AND X/D.

ii) The characteristics of the water surface layers around the pier surface affect the water ‘movement behavior which is changed due to the changes in the pier shape.

iii) The pressure and velocity values growth in polynomial progressive for each level Also, the water flow on the pier surface causes vortex lines leading from the pier tip.

iv) The same phenomenon and flow behaviors appear in the Iron Bridge case. The relative differences in the pressure and velocity belong to the different pier design.

v) From both cases, the researcher concludes that the amount of pressure distribution depends on the shape of the pier.

5.2 Future Work and Recommendations

The results observe many recommendations which considered as significant issues in future works:

i) It is recommended that to apply different surface area of the pier shapes which can reduce pressure forces. This can be achieved by enhance the pier design in both of side surface shape correlated with adding vortex reducers.

ii) To investigate the effect of front pier with respect to the back. This idea can observe a new pier design to reduce the vortex by a new back design.

REFERENCES

Aghaee, Y. and Hakimzadeh, H. 2010. Three dimensional numerical modeling of flow around bridge piers using LES and RANS. International Conference on Fluvial Hhydraulics, River Flow, 2: 211-218.

Alijani, F. and Amabili, M. 2014. Non-linear vibrations of shells: A literature review from 2003 to 2013. International Journal of Non-Linear Mechanics, 58: 233-257.

Atkins, K. 2015. Investigation into the flow behaviour of a NACA 0021 airfoil with leading edge undulations simulated with RANS in STAR-CCM+. Doctoral dissertation, The University of Manchester, 76 page, England.

Bouaani, M., Miquel, B. and Bouaanani, N. 2011. Practical dynamic analysis of structures laterally vibrating in contact with water. Computers & structures, 89 (23-24), 2195-2210.

Breusers, H. N. C. 1970. International Institute for Hydraulic and Environmental Engineering. Research Engineer Delft Hydraulics Laboratory, 7: 44-47.

Cakir, M. 2012. CFD study on aerodynamic effects of a rear wing/ spoiler on a passenger vehicle. MSc. Thesis, Santa Clara University, 61 page, California.

Carnacina, I., Leonardi, N. and Pagliara, S. 2019. Characteristics of flow structure around cylindrical bridge piers in pressure-flow conditions. Water, 11(11): 2240.

Chang, K. and Constantinescu, G. 2015. Numerical investigation of flow and turbulence structure through and around a circular array of rigid cylinders. Journal of Fluid Mechanics, 776: 161-199.

Charbeneau, R. J. and Holley, E. R. 2001. Backwater effects of bridge piers in subcritical flow. Austin, TX, USA: Center for Transportation Research, Bureau of Engineering Research, 512: 232-3138.

Chen, Z., Liu, L., Hu, Y., Ye, N., Shen, X.. and Wang, Y. 2021. Experimental on the protective performance of column bridge pier anti-scouring device. E3S Web of Conferences, 248: 2-7.

Ettema, R., Melville, B. W. and Constantinescu, G. 2011. Evaluation of bridge scour research: Pier scour processes and predictions, Transportation Research Board of the National Academies, 1: 112-132.

Ghobadian, R., Basiri, M. and Seydi Tabar, Z. 2018. Interaction between channel junction and bridge pier on flow characteristics. Alexandria Engineering Journal, 57: 2787-2795.

Hamidi, A. and Siadatmousavi, S. M. 2018. Numerical simulation of scour and flow field for different arrangements of two piers using SSIIM model. Ain Shams Engineering Journal, 9(4): 2415-2426.

Honarmand, M., Djavareshkian, M. H., Feshalami, B. F. and Esmaeilifar, E. 2019. Numerical simulation of a pitching airfoil under dynamic stall of low reynolds number flow. Journal of Aerospace Technology and Management, 11: 1-14.

Iaccarino, G. 2004. Simulation of Turbulent Flows, ME469B: Computational Methods in Fluid Dynamics Using Commercial CFD Codes. Standford University, 69 page, California.

Ipa, P. and Di, S. 2017. No Covariance structure anahysis of health-related indicators in the elderly at home with a fous on subjective health (January), 5: 3-9.

Jalal, H. K. 2019. Numerical study of optimum pier shape for safe bridge. MSc. Thesis, University of Kerbala, 62 page, Iraq.

Junichi Okado, A.Q., Tamaren, B., Naoko, S., Yoshinori, F. and Hoshi, D. 2003. No 主観的健康感を中心とした在宅高齢者における 健康関連指標に関する共分散構造分析 Title, Journal of Physical Therapy Science, 81: 19-30.

Lee, F. Z., Lai, J. S., Lin, Y. B., Chang, K. C., Liu, X. and Huang, C. C., 2018. Prediction of bridge pier scour depth and field scour depth monitoring. In E3S Web of Conferences EDP Sciences, 8: 3-10.

Malavasi, S. and Guadagnini, A. 2003. Hydrodynamic Loading on River Bridges, Journal of Hydraulic Engineering, 129: 854-861.

Malik, R. A. H. U. L. and Setia, B. A. L. D. E. V. 2014. Experimental study on behaviour of closely placed bridge pier models. In National Conference in Department of Civil Engineering National Institute of Technology Kurukshetra, 1: 3-7.

Melville, B. 2008. The physics of local scour at bridge piers. Proceedings of the 4th International Conference on Scour and Erosion, 1: 28-40.

Melville, B. W. 1975. Local Scour at Bridge Sites. PhD. Thesis, University of Auckland, 218 page, New Zealand.

Melville, B. W. and Coleman, S. E. 2000. Bridge scour, Water Resources Publications, Highlands Ranch, Colorado, 550 page, USA.

Melville, B. W. and Raudkivi, A. J. 1977. Flow characteristics in local scour at bridge piers. Journal of Hydraulic Research, 15(4): 373-380.

Mohammadi, M. 2008. Boundary shear stress around bridge piers. American Journal of Applied Sciences, 5(11): 1547-1551.

Moseley, P., Florez, J. M., Sonar, H. A., Agarwal, G., Curtin, W. and Paik, J. 2016. Modeling, design, and development of soft pneumatic actuators with finite element method. Advanced Engineering Materials, 18: 978-988.

Nasim, M. Damage modelling of reinforced concrete bridge piers under flood and log impact. PhD. Thesis, RMIT University, 97 page, Australia.

Nasim, M., Setunge, S., Zhou, S. and Mohseni, H. 2019. An investigation of water-flow pressure distribution on bridge piers under flood loading. Structure and Infrastructure Engineering, 15(2): 219-229.

Raisee, M., Jafari, A., Babaei, H. and Iacovides, H., 2010. Two-dimensional prediction of time dependent, turbulent flow around a square cylinder confined in a channel. International Journal for Numerical Methods in Fluids, 62(11): 1232-1263.

Ramos, P. X., Maia, R., Schindfessel, L., De Mulder, T. and Pêgo, J. P. 2016. Large Eddy Simulation of the water flow around a cylindrical pier mounted in a flat and fixed bed. 5: 8-16.

Richardson, E. V. and Davis, S. R. 2001. Evaluating scour at bridges (No. FHWA-NHI-01-001). United States. Federal Highway Administration. Office of Bridge Technology, 4: 340-383.

Saraf, A. K., Singh, M. P. and Chouhan, T. 2016. A Review on Aerodynamic Behavior of Airfoil when Surface Modified. International Journal of Scientific & Engineering Research, 7(3): 516-519.

Shen, H. W., Schneider, V. R. and Karaki, S. 1969. Local scour around bridge piers. Journal of the Hydraulics Division, 95(6): 1919-1940.

Shrestha, C. K. 2015. Bridge pier flow interaction and its effect on the process of scouring, PhD. Thesis, University of Technology, 394 page, Sydney.

Soğukpınar, H. 2017. Uçak Kanatlarında En İdeal Hücum Açısını Bulmak İçin 4 Rakamlı Naca 00xx Kan Profillerinin Nümerik Analizi. Uludağ University Journal of the Faculty of Engineering, 22: 169-178.

Sunny, N. A. and Mathai, A. 2017. Soil Structure Interaction Analysis of Multi Storey Building. International Journal For Science Technology And Engineering, 3: 67-70.

Suribabu, C. R., Sabarish, R. M., Narasimhan, R. and Chandhru, A. R. 2011. Backwater rise and drag characteristics of bridge piers under subcritical flow conditions. European Water, 36: 27-35.

Topczewski, Ł., Cieśla, J., Mikołajewski, P., Adamski, P. and Markowski, Z. 2016. Monitoring of Scour Around Bridge Piers and Abutments. Transportation Research Procedia, 14: 3963-3971.

Tsutsui, T. 2007. Fluid flow and fluid force acting on a cylindrical pier standing in a scour. Nihon Kikai Gakkai Ronbunshu, B Hen/Transactions of the Japan Society of Mechanical Engineers, Part B, 73(5): 1191-1197.

Tun, U. and Onn, H. 2018. The Effect of Angle of Attack Due to Airfoil Specification Requirements in Scope and Quality for the Award of the Degree of Masters of Engineering in Mechanical Engineering. Signature, 2: 40-63.

Type, P. and Elevation, F. 2016. Piers Table of Contents WisDOT Bridge Manual Chapter 13 – Piers, pp. 66-33, USA.

Vijayasree, B. A., Eldho, T. I., Mazumder, B. S. and Ahmad, N. 2019. Influence of bridge pier shape on flow field and scour geometry. International Journal of River Basin Management, 17: 109-129.

Wang, Y. H., Zou, Y. S., Xu, L. Q. and Luo, Z. 2015. Analysis of water flow pressure on bridge piers considering the impact effect. Mathematical Problems in Engineering, 8: 3-7.

Yang, Y., Melville, B. W., Macky, G. H. and Shamseldin, A. Y. 2019. Local scour at complex bridge piers in close proximity under clear-water and live-bed flow regime. Water, 11(8): 1520-1530.

Yang, Y., Melville, B. W., Sheppard, D. M. and Shamseldin, A. Y. 2018. Clear-water local scour at skewed complex bridge piers. Journal of Hydraulic Engineering, 144(6): 23-34.

Yuce, M. I. and Kareem, D. A. 2016. A numerical analysis of fluid flow around circular and square cylinders. Journal-American Water Works Association, 108(10): 546-554.

Zhai, Y. 2010. Time-Dependent Scour Depth Under Bridge-Submerged Flow. MSc. Thesis, University of Nebraska, 78 page, Lincoln.

CURRICULUM VITAE

Personal Information

Name and Surname : Haitham Fadhil Shihab SHIHAB

Education

MSc	Çankırı Karatekin University Graduate School of Natural and Applied Sciences Department of Civil Engineering	2019-Present
Undergraduate	Baghdad University College of Engineering	2000-2003